



UNIVERSIDADE FEDERAL DE SANTA CATARINA  
CAMPUS FLORIANÓPOLIS  
PROGRAMA DE PÓS-GRADUAÇÃO EM ENGENHARIA QUÍMICA

Guilherme Mascaldi de Figueiredo

**Development and synthesis of lanthanum-based perovskite-type catalysts for phenol  
removal from contaminated water under dark conditions**

Florianópolis-SC

2024

Guilherme Mascalchi de Figueiredo

**Development and synthesis of lanthanum-based perovskite-type catalysts for phenol removal from contaminated water under dark conditions**

Trabalho submetido ao Programa de Pós-Graduação em Engenharia Química da Universidade Federal de Santa Catarina para obtenção do título de Mestre em Engenharia Química.

Orientador: Prof. Dr. Adriano da Silva.

Co-orientador: Prof. Dr. Luciano da Silva (CIQA/México) e Prof. Dr. Antônio Augusto Ulson de Souza.

Florianópolis-SC

2024

Figueiredo, Guilherme Mascalchi de

Development and synthesis of lanthanum-based perovskite type catalysts for phenol removal from contaminated water under dark conditions / Guilherme Mascalchi de Figueiredo ; orientador, Adriano da Silva, coorientador, Luciano da Silva, coorientador, Augusto Ulson de Souza, 2024.

78 p.

Dissertação (mestrado) - Universidade Federal de Santa Catarina, Centro Tecnológico, Programa de Pós-Graduação em Engenharia Química, Florianópolis, 2024.

Inclui referências.

1. Engenharia Química. 2. Remediação. 3. Contaminação. 4. Caracterização. 5. Catálise. I. Silva, Adriano da. II. Silva, Luciano da. III. Souza, Augusto Ulson de. IV. Universidade Federal de Santa Catarina. Programa de Pós Graduação em Engenharia Química. V. Título.

Guilherme Mascalchi de Figueiredo

**Título:** Synthesis and development of lanthanum-based perovskite-type catalysts for phenol removal from contaminated water in environmental dark conditions

O presente trabalho em nível de mestrado foi avaliado e aprovado, em 24 de novembro de 2023, por uma banca examinadora composta pelos seguintes membros:

Prof. Adriano da Silva, Dr.

Universidade Federal de Santa Catarina - UFSC

Prof. Cristiano José de Andrade, Dr.

Universidade Federal de Santa Catarina - UFSC

Prof. Leandro Pellenz, Dr.

Instituto Federal de Brasília - IFB

Certificamos que esta é a **versão original e final** do trabalho de conclusão que foi considerada adequada para a obtenção do título de Mestre em Engenharia Química.

---

Coordenação do Programa de Pós-Graduação

---

Prof. Dr. Adriano da Silva

Orientador

Florianópolis-SC

2024.

A dedicatória deste trabalho é direcionada à muitas pessoas as quais a minha vida não seria a mesma, bem como esta obra muito menos seria possível. Contudo, dentre todas as pessoas importantes na minha vida, dedico esta obra àquela que faz parte dos meus sonhos acordados e enquanto durmo, por quem eu viajaria para a mais alta de todas as nuvens, atravessaria o mais longo dos desertos, ou mergulharia no mais profundo dos oceanos. À minha parceira de vida, Isabella Marques Torres de Souza.

Dedico esta obra também a minha família – meus avós, meus pais e meus irmãos. Meus avós pela transmissão de saberes, virtudes e valores passados, muitas vezes esquecidos na correria da vida, mas que sempre nos lembram de quem somos e de onde viemos. Meus pais pelo esforço, dedicação e força de vontade imensuráveis para educar a mim e meus irmãos, nos prover segurança, nos mostrar o caminho, e nos deixar cientes de que cabe a cada um de nós trilhá-lo, ainda que obstáculos inéditos existam e que tenhamos sempre a clareza de ultrapassá-los. Meu irmão pela parceria incontestável nos dias bons e ruins, na caminhada, compartilhando frustrações e conquistas. E, minha irmã, por sua eterna doçura, desde o dia em que nasceu.



## **AGRADECIMENTOS**

Primeiramente, gostaria de agradecer imensamente ao meu orientador, Prof. Dr. Adriano da Silva, o qual não só executou a função de orientador com maestria, mas que também exerceu as virtudes de compressão, atenção, companheirismo, apoio e resolução durante todo o período em que trabalhamos juntos. Professor, “muito obrigado!”.

Gostaria de agradecer também aos coorientadores, Prof. Dr. Antônio Augusto Ulson de Souza e Prof. Dr. Luciano da Silva, pela oportunidade. Aos amigos e colegas pesquisadores no LABMASSA-LABSIN, pelos dias de trabalho e trocas de conhecimento valiosas. Aos funcionários do LABMASSA-LABSIN, CTC e toda a UFSC, os quais propulsionam o ensino público brasileiro aos mais elevados patamares, e exercem a missão diária de levar o conhecimento a milhares de pessoas.

“AUDACES FORTUNA IUVAT”. (PUBLIUS VERGILIUS MARO, 70-19 AC)



## RESUMO

Nas últimas décadas, a crescente contaminação industrial de corpos d'água tem sido abordada por diversas técnicas de remediação, uma vez que águas contaminadas afetam a segurança, bem-estar e equilíbrio da sociedade. Métodos como Ultrassom, Ozônio, e Fotocatálise são exemplos de Processos Oxidativos Avançados (POAs) utilizados na degradação de contaminantes em meio aquoso, contudo, tais métodos possuem limitações quanto a sua aplicabilidade e performance. Perovskitas, por sua vez, são óxidos metálicos coordenados na fórmula  $ABO_3$ , onde A é um metal alcalino terra-rara, B é um metal de transição e O é um óxido. As perovskitas, portanto, são catalisadores metálicos porosos estáveis com elevado potencial oxidativo, os quais não necessitam de combinações de reagentes e outras formas de energia de ativação para promover a degradação efetiva destes contaminantes. O processo de degradação conduzido pelas perovskitas é iniciado pela atração e adsorção dos contaminantes presentes no meio para a sua superfície, prosseguindo-se para a oxidação destes contaminantes a substâncias menos nocivas, devido à sua superfície altamente carregada. Deste modo, o interesse no desenvolvimento de tecnologias alternativas de remediação de águas contaminadas utilizando-se as perovskitas têm crescido consideravelmente, visto sua aplicabilidade, versatilidade, performance, métodos de síntese, estruturas cristalinas estáveis e elevado potencial de oxidação. Tais atributos refletem a capacidade das perovskitas na degradação de contaminantes em diversos meios aquosos por meio de processos oxidativos avançados e catálise heterogênea. Neste trabalho, portanto, catalisadores do tipo perovskita ( $ABO_3$ ) com estrutura baseada em Lantânio foram sintetizados por meio do método Sol-Gel e rota EDTA-Citrato, com etapas de calcinação de até  $1000^\circ\text{C}$ . Os metais Ferro, Titânio e Níquel foram incluídos na formulação das perovskitas e tiveram como objetivo a verificação de diferenças na performance de degradação do contaminante-alvo deste estudo, o Fenol. Os ensaios preliminares de degradação de Fenol foram realizados com as perovskitas  $\text{LaFeO}_3$  (LFO),  $\text{LaTiO}_3$  (LTO) e  $\text{LaNiFeO}_3$  (LNFO), em condições escuras, pressão atmosférica, e temperatura ambiente, sem a adição de reagentes de ativação. Variações no período de duração dos experimentos preliminares também foram empregadas. Nestes testes, a performance de degradação dos catalisadores testados foi feita por meio de método desenvolvido para HPLC. Nos resultados preliminares, a perovskita  $\text{LaNiFeO}_3$  se destacou, observando-se uma degradação total de aproximadamente 50 % da concentração inicial de Fenol. Tais resultados serviram de critério de seleção para o aprofundamento de estudos na perovskita LNFE, e diferentes temperaturas de calcinação e condições de ensaio foram testadas para a perovskita. Dessa forma, três distintas perovskitas LNFE foram submetidas a outros dois ensaios de degradação, sendo o primeiro em condições escuras e temperatura e pressão ambientes, e o segundo em condições escuras e pressão ambiente, porém com temperatura de  $60^\circ\text{C}$ . Os resultados obtidos demonstraram uma eficiência de degradação de Fenol de aproximadamente 60 % no primeiro teste, e 80 % no segundo teste. Análises de caracterização (MEV, EDS, DRX, BET, FTIR e ZETA) foram realizadas nas três perovskitas LNFE sintetizadas e discutidas. Finalmente, o autor conclui que os materiais sintetizados neste estudo podem ser considerados como promissores no tratamento de águas contaminadas por Fenol, bem como que a temperatura de síntese e de ensaios de degradação influenciam significativamente na performance do tratamento.

**Palavras-chave:** Remediação. Contaminação. Caracterização. Catálise. Metais.

## RESUMO EXPANDIDO

### Introdução

Nas últimas décadas, a crescente contaminação industrial de corpos d'água tem sido abordada por diversas técnicas de remediação, uma vez que águas contaminadas afetam a segurança, bem-estar e equilíbrio da sociedade. Métodos como Ultrassom, Ozônio, e Fotocatálise são exemplos de Processos Oxidativos Avançados (POAs) utilizados na degradação de contaminantes em meio aquoso, contudo, tais métodos possuem limitações quanto a sua aplicabilidade e performance. Perovskitas, por sua vez, são óxidos metálicos coordenados na fórmula  $ABO_3$ , onde A é um metal alcalino terra-rara, B é um metal de transição e O é um oxido. As perovskitas, portanto, são catalisadores metálicos porosos estáveis com elevado potencial oxidativo, os quais não necessitam de combinações de reagentes e outras formas de energia de ativação para promover a degradação efetiva destes contaminantes. O processo de degradação conduzido pelas perovskitas é iniciado pela atração e adsorção dos contaminantes presentes no meio para a sua superfície, prosseguindo-se para a oxidação destes contaminantes a substâncias menos nocivas, devido à sua superfície altamente carregada. Deste modo, o interesse no desenvolvimento de tecnologias alternativas de remediação de águas contaminadas utilizando-se as perovskitas têm crescido consideravelmente, visto sua aplicabilidade, versatilidade, performance, métodos de síntese, estruturas cristalinas estáveis e elevado potencial de oxidação. Tais atributos refletem a capacidade das perovskitas na degradação de contaminantes em diversos meios aquosos por meio de processos oxidativos avançados e catálise heterogênea.

### Objetivos

O objetivo geral deste trabalho foi sintetizar materiais baseados em estruturas do tipo perovskita por meio do método EDTA-Citrato modificado, e testá-los na degradação de contaminantes fenólicos nas condições de ausência de luz, e, temperatura e pressão ambiente.

Com base neste escopo, objetivos específicos também foram determinados, como a caracterização química, física e microestrutural dos catalisadores sintetizados; a investigação da influência, se existente, de diferentes temperaturas e procedimentos de calcinação para a síntese dos catalisadores testados; a investigação do processo de degradação oxidativa dos contaminantes testados em condições escuras; e a avaliação das taxas de degradação e eficiência do processo em comparação aos dados observados na literatura.

### Metodologia

Neste trabalho, catalisadores do tipo perovskita ( $ABO_3$ ) com estrutura baseada em Lantânio foram sintetizados por meio do método Sol-Gel e rota EDTA-Citrato, utilizando-se os sais metálicos, ácido cítrico, EDTA e hidróxido de amônio, nas taxas molares 1;2:1,1:10, respectivamente. As condições de temperatura da mistura foi de 90°C por 2 horas, e as etapas de calcinação foram realizadas a 480°C para a primeira etapa, e temperaturas entre 700°C, 850°C e 1000°C na segunda etapa. Os metais Ferro, Titânio e Níquel foram incluídos na formulação das perovskitas e tiveram como objetivo a verificação de diferenças na performance de degradação do contaminante-alvo deste estudo, o Fenol. Os ensaios preliminares de degradação de Fenol foram realizados com as perovskitas  $LaFeO_3$  (LFO),  $LaTiO_3$  (LTO) e  $LaNiFeO_3$  (LNFO), em condições escuras, pressão atmosférica, e temperatura ambiente, sem a adição de reagentes de ativação. Variações no período de duração dos experimentos preliminares também foram empregadas. Os experimentos tiveram duração de 180 a 720 min, com uma concentração de 20 mg/L de fenol, 0.3 g de catalisador e intervalos de amostragem a

cada 30 min. Excepcionalmente para o teste com a perovskita LNFO, foi utilizada temperatura de 60°C. Nestes testes, a performance de degradação dos catalisadores testados foi feita por meio de método desenvolvido para HPLC.

As técnicas de caracterização utilizadas foram Microscopia Eletrônica de Varredura (MEV), Espectroscopia Dispersiva de Raio-X (EDS), Área Superficial (BET), Potencial Zeta (ZP), Difração Raio-X (DRX), Espectroscopia da Transformada de Fourier no Infravermelho (FTIR). Com relação às técnicas analíticas para a determinação das concentrações de Fenol, foi utilizada a Cromatografia Líquida de Alta Performance (HPLC).

### **Resultados e Discussão**

As perovskitas sintetizadas pelos métodos EDTA-Citrato resultaram em materiais de textura fina, semelhantes a um pó, com umidade imperceptível e coloração variada, entre marrom, cinza e preto, a depender da composição dos catalisadores. Ainda na etapa de síntese, verificou-se um rendimento aproximado de 3 g para cada catalisador. Nos resultados preliminares, observou-se eficiência de degradação de 32.8% (180 min) e 35.1% (720 min) para a perovskita LFO, e, 10.6% (180 min) e 18.3% (720 min) para a perovskita LTO. Para a perovskita LNFO, foram observadas degradações de 59.7% (700°C), 50.1% (850°C) e 49.9% (1000°C), para 180 min de duração do ensaio e 25°C. Nos ensaios com 60°C, a perovskita  $\text{LaNiFeO}_3$  se destacou, observando-se uma degradação 81.8% (700°C), 64.0% (850°C) e 55.9% (1000°C) para 180 min de duração de reação. Tais resultados serviram de critério de seleção para o aprofundamento de estudos na perovskita LNFE. Dessa forma, análises de caracterização (MEV, EDS, DRX, BET, FTIR e ZETA) foram realizadas nas três perovskitas LNFE sintetizadas. Os dados obtidos das análises de caracterização indicaram maior porosidade, distribuição dos poros, tamanho dos poros, área superficial, e carregamento elétrico de superfície para a perovskita sintetizada na temperatura de 700°C, quando comparada às demais (850°C e 1000°C). Adicionalmente, foi possível observar melhor distribuição dos metais presentes nas estruturas por meio das imagens geradas pelo MEV e EDS. Avaliando-se os resultados obtidos para o Potencial Zeta, contudo, observou-se maior potencial e condutividade para a perovskita de 850°C, o que pode indicar maiores propriedades coloidais e superfícies carregadas.

### **Considerações Finais**

É possível pontuar que o método EDTA-Citrato pode ser considerado como um método adequado para a síntese de catalisadores metálicos. Adicionalmente, com base nos resultados obtidos durante a pesquisa realizada, conclui-se que os materiais sintetizados neste estudo podem ser considerados como promissores no tratamento de águas contaminadas por fenol, bem como que a temperatura de síntese dos catalisadores testados e de condições de ensaios de degradação influenciam significativamente na performance de degradação do composto-alvo. Ainda, é possível sugerir que os mecanismos de formação de Espécies Reativas de Oxigênio (EROs) estão presentes, e que estes desempenham o papel principal na degradação dos contaminante estudado. Por fim, conclui-se que as análises de caracterização executadas são essenciais para suplementar as observações dos ensaios cinéticos de degradação quanto às características dos catalisadores estudados.

**Palavras-chave:** Remediação. Contaminação. Caracterização. Catálise. Metais.

## ABSTRACT

In recent decades, the increasing industrial contamination of water bodies has been addressed by various remediation techniques, since contaminated water affects the safety, well-being, and balance of society. Methods such as Ultrasound, Ozone, and Photocatalysis are examples of Advanced oxidation processes (AOPs) used in the degradation of contaminants in aqueous media, however, such methods have limitations regarding their applicability and performance. Perovskites are metal oxides coordinated in the  $ABO_3$  formula, where A is a rare-earth alkali metal, B is a transition metal, and O is an oxide. Perovskites, therefore, are stable porous metal catalysts with high oxidative potential, which do not require a combination of reactants and other forms of activation energy to promote the effective degradation of these contaminants. The degradation process conducted by perovskites is initiated by the attraction and adsorption of the contaminants present in the medium to its surface, proceeding to the oxidation of these contaminants to less harmful substances, due to its highly charged surface. Thus, the interest in the development of alternative technologies for remediation of contaminated water using perovskites has grown considerably, due to their applicability, versatility, performance, synthesis methods, stable crystal structures and high oxidation potential. Such attributes reflect the ability of perovskites to degrade contaminants in various aqueous media through advanced oxidation processes and heterogeneous catalysis. In this work, therefore, perovskite ( $ABO_3$ ) catalysts with lanthanum-based structure were synthesized by means of the Sol-Gel method and EDTA-Citrate route, with calcination steps of up to 1000 °C. The metals Iron, Titanium and Nickel were included in the formulation of the perovskites and aimed to verify differences in the degradation performance of the target contaminant of this study. the Phenol. Preliminary phenol degradation assays were performed with  $LaFeO_3$  (LFO),  $LaTiO_3$  (LTO) and  $LaNiFeO_3$  (LNFO) perovskites, under dark conditions, atmospheric pressure, and room temperature, without the addition of activation reagents. Variations in the duration of the preliminary experiments were also employed. In these tests, the degradation performance of the catalysts was made by means of a method developed for HPLC. In the preliminary results, the perovskite  $LaNiFeO_3$  stood out, observing a total degradation of approximately 50% of the initial phenol concentration. These results served as a selection criterion for further studies on LNFE perovskite, and different calcination temperatures and test conditions were tested for perovskite. Thus, three different LNFE perovskites were subjected to two other degradation tests, the first in dark conditions and ambient temperature and pressure, and the second in dark conditions and ambient pressure, but with a temperature of 60 °C. The results obtained demonstrated a phenol degradation efficiency of approximately 60% in the first test, and 80% in the second test. Characterization analyses (MEV, EDS, DRX, BET, FTIR and ZETA) were performed on the three LNFE perovskites synthesized and discussed. Finally, the author concludes that the materials synthesized in this study can be considered as promising in the treatment of water contaminated by Phenol, as well as that the synthesis temperature and degradation tests significantly influence the treatment performance.

**Keywords:** Remediation. Contamination. Characterization. Catalysis. Metals.

## LISTA DE FIGURAS

FIGURE 1. SOURCES OF PHENOLIC COMPOUNDS IN WATER AND ITS PATHWAYS. MODIFIED FROM RAZA, ET AL., 2019; AND BIBI, ET AL., 2023.....	16
FIGURE 2. PEROVSKITE-TYPE $ABO_3$ STRUCTURE. MODIFIED FROM SUN, 2022. ....	25
FIGURE 3. PHENOL MOLECULE. MODIFIED FROM GUO, ET AL., 2020. ....	31
FIGURE 4. SYNTHESIS STEPS OF $LaFeO_3$ PEROVSKITE. ....	41
FIGURE 5. FIRST EXPERIMENT RESULTS FOR PHENOL DEGRADATION PERFORMANCE BY $LaFeO_3$ . ....	43
FIGURE 6. SECOND EXPERIMENT RESULTS FOR PHENOL DEGRADATION PERFORMANCE BY $LaFeO_3$ . ....	16
FIGURE 7. SYNTHESIS STEPS OF $LaTiO_3$ PEROVSKITE. ....	18
FIGURE 8. FIRST EXPERIMENT RESULTS FOR PHENOL DEGRADATION PERFORMANCE BY $LaTiO_3$ .....	20
FIGURE 9. SECOND EXPERIMENT RESULTS FOR PHENOL DEGRADATION PERFORMANCE BY $LaTiO_3$ .....	21
FIGURE 10. SYNTHESIS STEPS OF $LaNiFeO_3$ PEROVSKITES AT DIFFERENT CALCINATION TEMPERATURES.....	24
FIGURE 11. FIRST EXPERIMENT RESULTS FOR PHENOL DEGRADATION PERFORMANCE BY $LaNiFeO_3$ PEROVSKITES. ....	25
FIGURE 12. SECOND EXPERIMENT RESULTS FOR PHENOL DEGRADATION PERFORMANCE BY $LaNiFeO_3$ PEROVSKITES. ....	27
FIGURE 13. SEM PICTURES OBTAINED AT 1000X AND 2500X ZOOM FROM $LaNiFeO_3$ PEROVSKITE STRUCTURE.....	29
FIGURE 14. SEM PICTURE FROM $LaNiFeO_3$ AND EDS ANALYSIS. ....	31
FIGURE 15. EDS INTENSITY SPECTRUM FOR $LaNiFeO_3$ PEROVSKITE.....	32
FIGURE 16. BET RESULTS FOR $LaNiFeO_3$ PEROVSKITES. ....	33
FIGURE 17. X-RAY DIFFRACTION DATA FOR $LaNiFeO_3$ PEROVSKITES.....	37
FIGURE 18. FTIR RESULTS FOR $LaNiFeO_3$ PEROVSKITE CALCINED AT 700 °C. ....	38

FIGURE 19. FTIR RESULTS FOR $\text{LANiFeO}_3$ PEROVSKITE CALCINED AT $850^\circ\text{C}$ . .....	38
FIGURE 20. FTIR RESULTS FOR $\text{LANiFeO}_3$ PEROVSKITE CALCINED AT $850^\circ\text{C}$ . .....	39

## LISTA DE TABELAS

TABLE 1. CHEMICAL PRODUCTS UTILIZED IN THE SYNTHESIS AND ITS SPECIFICATIONS. ....	33
TABLE 2. TARGET POLLUTANT SPECIFICATIONS.....	33
TABLE 3. DEGRADATION EXPERIMENTS PARAMETERS. ....	37
TABLE 4. CHEMICAL REAGENTS QUANTITIES FOR SYNTHESIS PROCESS OF $\text{LaFeO}_3$ .....	40
TABLE 5. CHEMICAL REAGENTS QUANTITIES FOR SYNTHESIS PROCESS OF $\text{LaTiO}_3$ .....	17
TABLE 6. CHEMICAL REAGENTS QUANTITIES FOR SYNTHESIS PROCESS OF $\text{LaNiFeO}_3$ .....	23
TABLE 7. EDS DISTRIBUTION DATA FOR $\text{LaNiFeO}_3$ PEROVSKITE. ....	32
TABLE 8. ZETA POTENTIAL RESULTS FOR $\text{LaNiFeO}_3$ PEROVSKITES. ....	34

## LISTA DE EQUAÇÕES

EQUATION 1.....	20
EQUATION 2.....	20
EQUATION 3.....	22
EQUATION 4.....	22
EQUATION 5. HPLC MEASUREMENTS CONVERSION TO PHENOL CONCENTRATION IN MG/L.....	43



## INDICE

<b>1.</b>	<b>INTRODUCTION .....</b>	<b>15</b>
1.1	OBJECTIVES.....	18
<b>1.1.1</b>	<b>General Objective .....</b>	<b>18</b>
<b>1.1.2</b>	<b>Specific Objectives .....</b>	<b>18</b>
1.2	STRUCTURE OF THE DISSERTATION .....	18
<b>2</b>	<b>LITERATURE REVIEW .....</b>	<b>19</b>
2.1	ADVANCED OXIDATION PROCESSES(AOPs) .....	19
<b>2.1.1</b>	<b>Photo-Oxidation Processes.....</b>	<b>20</b>
2.1.1.1	<i>Photo-Fenton Reaction .....</i>	20
2.1.1.2	<i>Heterogeneous Photocatalysis.....</i>	21
<b>2.1.2</b>	<b>Dark-Oxidation Processes.....</b>	<b>21</b>
2.1.2.1	<i>Fenton-like Processes.....</i>	21
2.1.2.2	<i>Ultrasound.....</i>	22
2.1.2.3	<i>Ozonation.....</i>	22
2.1.2.4	<i>Heterogeneous catalysis in dark conditions .....</i>	23
2.2	HETEROGENEOUS CATALYSTS.....	24
<b>2.2.1</b>	<b>Metal Oxide Based Catalysts .....</b>	<b>24</b>
2.2.1.1	<i>Iron (Fe) based catalysts .....</i>	27
2.2.1.2	<i>Titanium (Ti)-based catalysts .....</i>	28
2.2.1.3	<i>Lanthanum (La)-based catalysts .....</i>	28
2.3	SYNTHESIS METHOD.....	30
2.4	TARGET CONTAMINANT.....	30
<b>2.4.1</b>	<b>Phenol .....</b>	<b>31</b>
<b>3</b>	<b>MATERIAL AND METHODS .....</b>	<b>32</b>
3.1	CHEMICAL REAGENTS .....	32

3.2	CHARACTERIZATION TECHNIQUES .....	35
3.2.1	<b>Scanning Electron Microscopy (SEM) and Energy Dispersive X-Ray Spectroscopy (EDS).....</b>	<b>35</b>
3.2.2	<b>Surface Area (BET).....</b>	<b>35</b>
3.2.3	<b>Zeta Potential (ZP) .....</b>	<b>35</b>
3.2.4	<b>X-Ray Diffraction (XRD).....</b>	<b>36</b>
3.2.5	<b>Fourier Transform Infrared Spectroscopy (FTIR).....</b>	<b>36</b>
3.3	ANALYTICAL TECHNIQUES .....	37
3.3.1	<b>High Performance Liquid Chromatography (HPLC).....</b>	<b>37</b>
3.4	EVALUATION OF CATALYTIC ACTIVITY.....	37
3.4.1	<b>Degradation Kinetics .....</b>	<b>37</b>
4	<b>RESULTS AND DISCUSSION.....</b>	<b>39</b>
4.1	LaFeO <sub>3</sub> PEROVSKITE-TYPE LANTHANUM BASED CATALYST .....	39
4.1.1	<b>Catalyst Synthesis .....</b>	<b>40</b>
4.1.2	<b>Degradation Kinetics and Catalytic Activity .....</b>	<b>41</b>
4.1.2.1	<i>Catalytic Performance.....</i>	<i>42</i>
4.2	LaTiO <sub>3</sub> PEROVSKITE-TYPE LANTHANUM BASED CATALYST .....	17
4.2.1	<b>Catalyst Synthesis .....</b>	<b>17</b>
4.2.2	<b>Degradation Kinetics and Catalytic Activity .....</b>	<b>19</b>
4.2.2.1	<i>Catalytic Performance.....</i>	<i>19</i>
4.3	LaNiFeO <sub>3</sub> PEROVSKITE-TYPE LANTHANUM BASED CATALYST .....	22
4.3.1	<b>Catalyst Synthesis .....</b>	<b>22</b>
4.3.2	<b>Degradation Kinetics and Catalytic Activity .....</b>	<b>24</b>
4.3.2.1	<i>Catalytic Performance.....</i>	<i>25</i>
4.3.3	<b>Characterization Techniques.....</b>	<b>28</b>
4.3.3.1	<i>Scanning Electron Microscopy (SEM) and Energy Dispersive X-Ray Spectroscopy (EDS)</i>	<i>28</i>

4.3.3.2	<i>Surface Area (BET)</i> .....	32
4.3.3.3	<i>Zeta Potential (ZP)</i> .....	33
4.3.3.4	<i>X-Ray Diffraction (XRD)</i> .....	35
4.3.3.5	<i>Fourier Transform Infrared Spectroscopy (FTIR)</i> .....	37
<b>5</b>	<b>CONCLUSIONS AND FINAL CONSIDERATIONS</b> .....	<b>40</b>
<b>6</b>	<b>SUGGESTIONS FOR FUTURE WORK</b> .....	<b>41</b>
<b>7</b>	<b>REFERENCES</b> .....	<b>42</b>

## 1. INTRODUCTION

Perovskite minerals are oxides that are usually coordinated in the formula  $ABO_3$ , where A is a rare earth alkaline metal, B is a transition metal, and O is an oxide. There are several different formulas that can be synthesized through metal complexation processes that will result in stable perovskite-like materials. The growing interest in this material for scientific research and industrial applications is based on its striking characteristics: a defined and stable structure, oxidation potential, and versatility (LI, et al., 2012; ZHU, H. et al., 2015; TANG, et al., 2019).

In the last century, water contamination through industrial waste has grown exponentially, causing irreversible damage to populations, natural systems, and economies. Water is the most fundamental molecule for all living-organisms on Earth, and it sustains all the existing life-systems ever studied. Naturally, humans exclusively depend on the access to clean water to survive and thrive (MAINALI, 2020; NOROUZI, et al., 2020; COELHO, et al., 2022).

The contamination of surface water and groundwater systems can negatively impact all industries, causing severe economic issues, and it has been considered a global crisis (NOROUZI, et al., 2020).

Arguably, many factors threaten clean water security, however, accelerated socioeconomic growth paired with the intense development of industrial services has had the greatest negative contribution to date, due to its high demand for water supply, and most importantly, to the irresponsible discharge of contaminated effluents and wastewater into natural systems such as lakes, rivers, ponds, and groundwater. Furthermore, there is growing evidence that climate change and a more intense global warming will also compose the main factors that threaten water security (WETCHAKUN, et al., 2018; NOROUZI, et al., 2020; DUTTA, et al., 2021).

Hence, there is an unstoppable urgency to mitigate the water contamination crisis, by creating stricter regulations, smarter systems, effluents recycling methods and, most of all, pollution reduction of recharge areas, such as aquifers, lakes, and rivers, in order to safeguard life on Earth. (ANNAMALAI, et al., 2022; BIBI, et al., 2023).

Among the various contaminants often found in contaminated waters, phenolic compounds such as Phenol, bisphenol A, 2-Chlorophenol, 4-Chlorophenol, and Nitrophenols are the main toxic chemicals often present in these systems (KARIM, et al., 2021; ANNAMALAI, et al., 2022).

The organic compound evaluated in this work (phenol) presents dangerous environmental effects in many forms, and due to its toxicity, it is extremely carcinogenic to humans, causing mutagenic effects, as well as immunological disorders (VAIANO, et al., 2018; ANNAMALAI, et al., 2022).

Phenol ( $C_6H_5OH$ ) is often found in the environment as a building block molecule that allows the conformation of more complex organic molecules. As such, when phenol is paired with halogens for their electrochemical properties, even more harmful molecules are created, such as 2-Chlorophenol (2-CP), which has neurotoxic effects and can cause DNA damage. Therefore, it is essential to incorporate more robust treatments into wastewater treatment systems as well as surface water and groundwater, in order to ensure effective water remediation (ALMASI, et al., 2021; BIBI, et al., 2023).

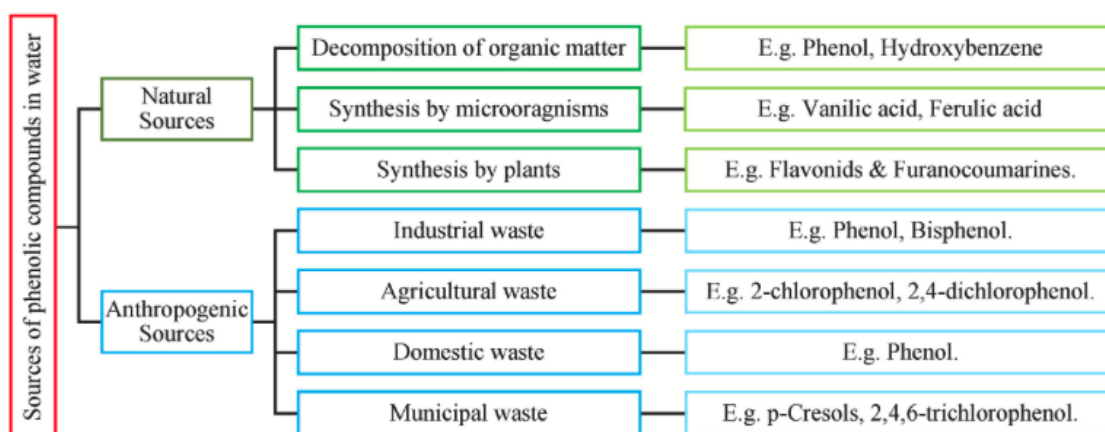


Figure 1. Sources of phenolic compounds in water and its pathways. Modified from RAZA, et al., 2019; and BIBI, et al., 2023.

In that sense, Advanced Oxidation Processes (AOPs) are promising technologies for the treatment of various industrial effluents and remediation of contaminated waters. AOPs are chemical processes that remove and oxidize soluble organic contaminants from water by the use of in-situ applications of strong oxidants. Such processes may combine several types of oxidants, being ozone and hydroxyl radicals the most commonly used reactive oxygen species, however its treatment efficiency alone is not entirely significant. Therefore, several chemicals are often paired with UV-lamps for stronger activation, or with chemicals such as hydrogen peroxide, in order to increase oxidation capacity.

Ozone has low solubility and stability in acidic and neutral environments; thus, the formation of hydroxyl radicals is fairly slow, paired up with hydrogen peroxide or UV-lamps, it generates more hydroxyl radicals, resulting in higher oxidation levels.

Catalysts, for instance, are usually metallic oxides that can provide great oxidation power with or without the combination of chemicals and other forms of activation energy. Metallic oxides, such as perovskites, are stable porous catalysts that will primarily induce the adsorption of these contaminants into their surface, and consequently oxidize these contaminants into less harmful and smaller molecules, due to its highly charged surface.

In Esplugas, et al., 2002 work, several AOPs with different UV, metals, ozone, and hydrogen peroxide combinations, were evaluated, including photocatalysis processes for the oxidation of phenol in aqueous medium with an initial concentration of 100 mg/L. Among these, the Fenton-based process reported the fastest removal rates for phenol in wastewater with a removal efficiency ranging from 32 to 100% within 9 min.

Photocatalysis, for instance, had the longest period of degradation (150 min) where the removal efficiency ranged between 42% and 77%. However, the authors stated that from an economical point of view, ozonation was found to be more cost-effective (ESPLUGAS et al., 2002).

In another study,  $\text{LaBO}_3$  (B=Cu, Fe, Co, Ni, Mn) perovskites were tested on the efficiency of phenol oxidation and conversion from phenol to  $\text{CO}_2$  and  $\text{H}_2\text{O}$ . Compared with Fenton-like processes, perovskites have shown higher versatility on pH variations, necessity of catalyst regeneration and its deactivation in the presence of complexing substances (TARAN, et al., 2016). Several studies have demonstrated the ability of perovskites in the degradation of organic contaminants (ROJAS-CERVANTES, et al., 2019; WANG, et al., 2021). However, few scientific publications focused on the utilization in dark catalysis, that is, in the absence of any type of light irradiation, in which one of the greatest assets of is the considerably lower energy expenditure and related costs when compared to photocatalysis.

Therefore, the study of perovskites for the degradation of phenolic compounds in dark conditions as a potential strategy to address the long-lasting and still growing problematic scenario of water contamination is of great importance. This work intends to provide data and discuss this strategy with lanthanum-based perovskites and propose a new and cost-effective treatment through the use of AOPs.

## 1.1 OBJECTIVES

### 1.1.1 General Objective

Synthesize heterogeneous catalysts based on a perovskite-type structure and apply it on the degradation of phenolic organic contaminants under dark conditions, at room temperature and pressure.

### 1.1.2 Specific Objectives

- Synthesize materials based on perovskite structures by means of the EDTA-citrate (or Pecini) complexation route;
- Evaluate the influence, if any, of different calcination temperatures for the synthesis of the studied catalysts;
- Characterize chemically, physically, and microstructurally the synthesized catalysts;
- Investigate the oxidative degradation of different organic contaminants in conditions of absence of light; and
- Evaluate the degradation rate and efficiency of the catalysts produced in this work in comparison to catalysts reported in literature.

## 1.2 STRUCTURE OF THE DISSERTATION

The present research is organized into 5 chapters. The content of each chapter is summarized below:

- Chapter 1: introduces the subject matter of research, providing understanding of the motivations and objectives of this research project, as well as the organization of the dissertation.
- Chapter 2: presents the literature review efforts, in which several advanced oxidation processes commonly adopted for water treatment are addressed and discussed, including the verified milestones in heterogeneous catalysis in dark conditions associated with metal oxides and perovskite-type catalysts. In addition, the toxicity, fate, and origin of the target phenolic contaminants are also discussed.
- Chapter 3: discusses the catalysts synthesis processes, steps, and the various characterization techniques utilized on the studied materials throughout this work.
- Chapter 4: presents the results and discusses the main findings of this dissertation.
- Chapter 5: reports the conclusions and final considerations of this work and provides insights for future studies on the subject matter.

## 2 LITERATURE REVIEW

### 2.1 ADVANCED OXIDATION PROCESSES (AOPS)

Advanced oxidation processes (AOPs) involve several chemical processes designed to remove and degrade hazardous chemicals and pollutants from water sources. These chemicals commonly involve variations of hydrogen species, such as hydrogen peroxide, super oxides, and ozone. Catalysts composed by metallic oxides are also a very important group in these processes, which have been reported as great components of such systems, offering striking advantages among others (MIAO, et al., 2017; AIZAT, et al., 2018).

The main mechanism of reaction among these chemicals is through the release of ROS into the target medium. The hydroxyl radical ( $\text{OH}^\cdot$ ) is often referred to as the most important oxidizer in such processes, due to its high oxidation potential of 2.81 eV (MIAO, et al., 2017).

Following the release of such species, organic molecules in the medium tend to break bonds and form new molecules in response to a new energetic balance, which allows the non-selective reaction, degradation, and complete mineralization of these molecules into  $\text{CO}_2$  and  $\text{H}_2\text{O}$ .

As such, AOPs can either be enhanced by photoenergy or operate in the absence of light. On photo-oxidation, oxidants are activated and stimulated by UV-lighting in order to provide a greater hydroxyl radicals formation. Photo-Fenton-like processes, photo-ozonation and heterogenous photo-catalysis are two great examples of photo-oxidation treatments (MIAO, et al., 2017; HAMMOUDA, et al., 2019).

In parallel, dark oxidation does not require the use of stimulants or activators such as UV-lighting, as it is operated in the absence of light. This classification includes processes such as Fenton reaction, ozonation, ultrasound, and dark catalysis (HAMMOUDA, et al., 2019; ROJAS-CERVANTES, et al., 2019).

As previously mentioned, this work has dark catalysis as the main AOP for the oxidation and degradation of phenol. Thus, the following sections provide literature knowledge on AOPs in both categories: photo-oxidation and dark-oxidation. This is intended to provide contextualization on the matter for further understanding of the key differences, advantages, and disadvantages of these processes on the remediation of contaminated waters.



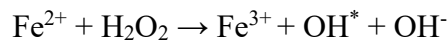
## 2.1.1 Photo-Oxidation Processes

### 2.1.1.1 Photo-Fenton Reaction

Fundamentally, the Fenton reaction involves the reaction of Fe (II) with hydrogen peroxide, resulting in the production of hydroxyl and hydroxyl radicals (Equations 1 and 2). However, in the Photo-Fenton process, as previously introduced, photoenergy is also utilized as an activation method in the photocatalysis of hydrogen peroxide, further dissociating such molecules in order to produce more hydroxyl radicals. The use of photoenergy also improves the rate of conversion from Fe (III) to Fe (II). These sources of light may be UV, sunlight, or IR-light. Naturally, due to the greater energy transported by lower wavelengths, UV-Fenton processes will generate the greatest results (HAMMOUDA, et al., 2019; DOWD, et al., 2020; WANG, et al., 2021).

The Fenton reaction is described by the Equations, below:

Equation 1.

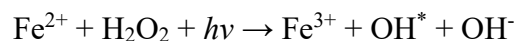


Equation 2.

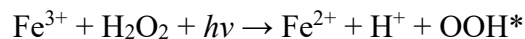


The Photo-Fenton reaction is described by the Equations, below:

Equation 3.



Equation 4.



The photo-Fenton reactions occur with the photolysis of hydrogen peroxide and its reaction with Fe (II), resulting on the production of hydroxyl radicals. The formed Fe (III) is further reduced by the hydrogen peroxide, producing more hydroxyl radicals. These reactions, however, require the control of a few parameters, such as pH control in an acidic to neutral range, with very low variability, and the residue that tends to accumulate by the reduction of iron. These aspects are considered as disadvantages to the Photo-Fenton method, even though

it has a significant efficiency in degrading several organic contaminants (CAI, et al., 2016; GARCIA-MUNOZ, et al., 2020).

Additionally, one way to increase Photo-Fenton's reaction and control the acidic-neutral characteristic of the reaction, is to rejuvenate the solution with  $H_2O_2$ . Nevertheless, this adds another step into the operation of this process, what may increase its necessity for control (GARCIA-MUNOZ, et al., 2020).

#### *2.1.1.2 Heterogeneous Photocatalysis*

Heterogenous catalysis is considered as the process of using catalysts activated by photoenergy, that is, with the presence of light, in order to enhance its catalytic activity. This is achieved by the incidence of light onto the surface of the catalysts, following the absorption of energy greater than the catalysts bandgap, forcing the release of electrons ( $e^-$ ), and charging its surface with excited particles (KUMAR, et al., 2017; WANG, et al., 2021).

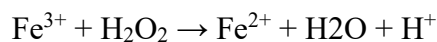
With this activation process, several oxidizing species are also formed, such as hydroxyl radicals and oxides, that will consequently react with the contaminants present in the solution. Naturally, however, as discussed on the aspects of Photo-Fenton processes, heterogenous catalysis requires energy for the operation of light sources, and its efficiency is directly linked with the amount of energy provided by such source. Other essential requirements are the catalysts distribution within the contaminated solution and the necessity of close contact with the contaminant for greater oxidation, which is achieved by constant agitation. Nonetheless, this technique is widely used for the degradation of organic chemicals, due to its ease of operation, stability, and possibility of catalyst reuse cycles (GARCIA-MUNOZ, et al., 2020; WEI, et al., 2021).

### **2.1.2 Dark-Oxidation Processes**

#### *2.1.2.1 Fenton-like Processes*

Fenton's reaction in dark conditions requires the use of hydrogen peroxide to induce the reaction between Fe (III) hydroxide, producing Fe (II) and hydroxyl radicals. Fe (II) produced further reacts with the residual  $H_2O_2$ , producing Fe (III) and more hydroxyl radicals. Both reactions take place as long as  $H_2O_2$  is replenished in the solution. The radicals then will oxidize the organic contaminants present in the solution (RAHIM POURAM, et al., 2014; ROJAS-CERVANTES, et al., 2019). The Fenton reaction with  $H_2O_2$  in dark conditions is presented in the Equations below:

Equation 3.



Equation 4.



Besides the rejuvenation of  $\text{H}_2\text{O}_2$ , pH adjustment to acidic conditions is also a requirement of this process since degradation rates were found to be greater in these experiments. Furthermore, as presented on the Photo-Fenton process, the formation of residual material derived from the reactions are considered a disadvantage to the process, and limitation for large-scale operations (RUSEVOVA, et al., 2014; WANG, et al., 2018).

#### 2.1.2.2 Ultrasound

In ultrasound process, as the name suggests, ultrasound frequency (20 Hz – 1000 KHz) is utilized for the degradation of organic pollutants in the absence of light. This process is carried out by applying ultrasound into a contaminated solution, causing microbubbles throughout the solution, trapping the contaminants molecules, and inducing high pressures and temperature in the internal space of such bubbles. This phenomenon consequently causes the formed bubbles to collapse due to the constant incidence of ultrasound, resulting in bond breaking through thermal dissociation, and, ultimately, the formation of hydroxyl radicals (KIDAK, et al., 2006; SINGH, et al., 2016).

However, in terms of operation effectiveness, this process requires high amounts of energy in order to produce the necessary sound frequency. Additionally, microbubbles non-uniform distribution can lead to uncomplete degradation and further mineralization of the target contaminants, making it difficult for scale-up. Due to these factors, other AOPs are often preferred or paired with Ultrasound, in order to overcome such limitations and achieve greater efficiency (RAYAROTH, et al., 2016; LU, et al., 2021).

#### 2.1.2.3 Ozonation

In this particular process, ozone ( $\text{O}_3$ ) reacts with the aqueous medium and its compounds, resulting in the generation of several chemical species ( $\text{HO}_2^-$ ,  $\text{O}_2^-$ ,  $\text{O}_3^-$ , and  $\text{O}^-$ ). However, the main ROS formed in such reaction is the hydroxyl radical,  $\text{OH}^\cdot$ . Due to its

characteristics, ozonation has been largely applied on water treatment, as well as on the immobilization and degradation of contaminants (DAI, et al., 2018; WANG, et al., 2021). Although, according to data reported in literature, the oxidative reaction rates are fairly slow when compared to other methods, resulting in incomplete mineralization of the target contaminants. Therefore, ozonation is usually paired with other types of treatment, due to its reaction rate and non-selective characteristics.

Moreover, as presented for a few of the above discussed methods, energy consumption, pH control, reagent replenishment, and difficult operation are the main factors that offset this treatment and limits its application in higher scales (WANG, et al., 2020; ISSAKA, et al., 2022).

#### *2.1.2.4 Heterogeneous catalysis in dark conditions*

Heterogeneous catalysis corresponds to the utilization of solid catalysts for the degradation of aqueous or gaseous phase contaminants, that is, different state materials. Thus, the reactions between the catalysts and the target compounds take place on the surface, and/or inside the pores of the catalyst, in the absence of light. As such, adsorption plays a big role on the operation of this process, in which highly porous catalysts will usually present more catalytic activity. However, this is also directly linked to another main process, which is the reaction of contaminants with the catalysts charged surface (BESEGATTO, et al., 2021; WANG, et al., 2021).

Fundamentally, heterogeneous catalysis involves the following steps: a. contact between the contaminant and the catalyst surface; b. adsorption of the contaminant into the pores of the catalyst; c. reaction of the adsorbed phase with the catalyst; d. desorption of the generated byproducts into the medium; and e. release of byproducts into the solution.

As previously mentioned, the reaction mechanisms between catalyst-contaminant and its performance are linked to the catalyst surface physical and electrochemical characteristics. Several reaction mechanisms may take place in the degradation of such contaminants, such as surface electron transfer, Mars-van Krevelen reaction, radical chain oxidation, and the thermal dissociation of molecules, if heat is applied. Consequently, the final outcome of such reaction mechanisms results in the formation of ROS, such as hydroxyl radicals, which will subsequently also react with the remaining contaminant molecules (CHEN, et al., 2020; LUO, et al., 2022).

Naturally, many factors influence the reactions performance, such as uniform distribution of the catalyst, close contact with the contaminant, and temperature. Nevertheless, this type of treatment stands itself due to its advantages when compared to others, which are the ease of operation and control, energy expenditure, the use of less chemical reagents, and the possibility of catalyst recycle/reuse (LUO, et al., 2022).

## 2.2 HETEROGENEOUS CATALYSTS

As presented above, catalysts are components that essentially decrease the activation energy of chemical reactions. The greatest difference between homogenous and heterogenous catalysts are that the first is applied to same state solutions, such as liquid-liquid, whilst the latter is based on different state substances applied to different state solutions (aqueous or gaseous). Heterogenous catalysts, however, offer a set of advantages related to the degradation of organic contaminants when compared to homogenous catalysts. These advantages are mostly due to the recovery of the catalyst after the treatment process, resulting in lower operational costs, higher scalability, and a defined structure that provides a higher reaction rate.

In this sense, metal oxide-based catalysts are on the forefront of catalytic activity in heterogenous catalysis, due to their stable structure, operation, and treatment performance.

As such, this next section presents a review of the literature focusing on advances in the synthesis of metal oxide-based catalysts in dark environmental conditions, and its application in the degradation of organic compounds, which is the subject matter of this dissertation.

### 2.2.1 Metal Oxide Based Catalysts

Metal oxide-based catalysts are known chemicals employed in several water treatment and sanitation processes. The most commonly applied catalysts are single oxides, such as iron oxides, titanium oxides, aluminum, magnesium, chromium, among others. However, mixed metal oxides have been subject of attention when it comes to the enhancement of treatment processes, in which it is possible to utilize further metallic combinations with relatively ease and versatility (ROJAS-CERVANTES, et al., 2019; WANG, et al., 2020; WANG, et al., 2021).

As previously mentioned in Chapter 1. Introduction, perovskites-type catalysts are a major example of mixed metal oxide-based catalysts in heterogenous catalysis. Namely, perovskite is a naturally occurring rare mineral composed by the formula  $\text{CaTiO}_2$ . It has a stable

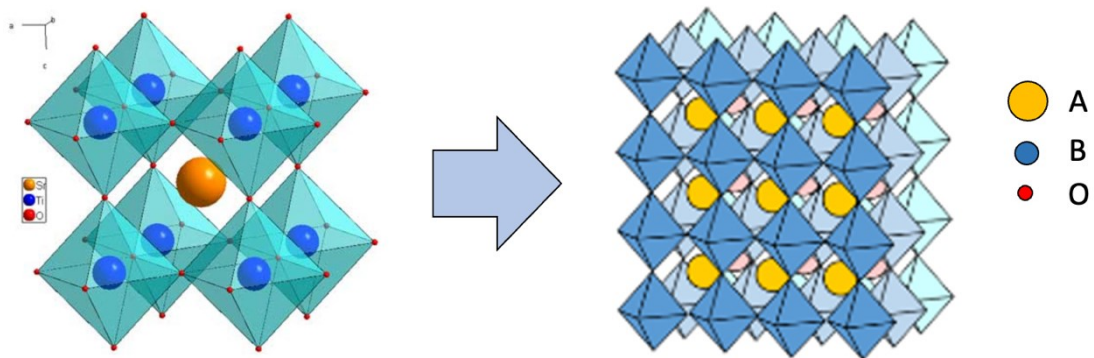
cubic structure, and well established crystalline structure. It is formed in Earth's mantle, mainly through the cooling of igneous ultramafic (very low  $\text{SiO}_2$  content) rocks (DAS-KANDIMALLA., 2017).

Due to their stable formula and advantages, perovskite-type materials were synthesized for scientific-research purposes, as well as for its application in industrial processes, especially catalysis. Perovskite-type structures are composed by the general formula  $\text{ABX}_3$ , in which A is a large cation, which can vary from alkaline metals (Na, K), rare-earth (Mg, Ca, Sr, Ba, Cu), and lanthanides (La). B, for instance, are smaller cations and transition metals, such as Ni, Fe, and Ti, and ultimately, X is often composed by an oxygen anion, however a few modifications might occur, with the inclusion of halogen ions, such fluorine ( $\text{F}^-$ ), chloride ( $\text{Cl}^-$ ), and iodine (I) (ZHU, et al., 2015; CHEN, et al., 2016).

In this aspect, many sub-classifications exist based on the elements utilized, as well as the elements employed. Generally, two main categories exist: Halide perovskite-type materials, and Oxide perovskite-type materials. The first, utilizes halogens to bond the cations, and the latter, utilizes oxygen.

When it comes to mixed oxides, the perovskite-type structure consists of  $\text{ABO}_3$ . The Figure 2 below depicts the perovskite structure, as well as its coordination characteristics.

Figure 2. Perovskite-type  $\text{ABO}_3$  structure. Modified from SUN, 2022.



As shown above, it is possible to verify that the perovskite-type structure is composed by octahedrons that are bonded and organized into a cubic structure. The single octahedron consists of the B element, such as the rare-earth metals (Ni, Fe, Ti) positioned in the center, and coordinated by 6 sites, all occupied by oxides. Each of these octahedrons, are bonded to the A

elements (La, Mg, Ca, Sr, Cu) and oriented into an octahedral cube coordination with 12 sites. Observing the formed cubic structure, it is also possible to verify that the element A occupies the center of the cube, with the B element occupying the 8 vertices, and oxides occupying the 12 sites of each edge (ZHU, et al; 2015; DAS-KANDIMALLA, 2017).

Even though this structure represents the ideal perovskite-type structure, a few variations in its organization also exists. This is due to the mixing of several other elements in A and B sites, especially B, in which different cations might have different sizes, that is, their ionic radius, what usually causes the necessity of coordination reshaping in order to maintain a stable structure.

This phenomenon might create modifications that will result in changes in its original cubic structure, making it rhombohedral, orthorhombic, or tetragonal. Therefore, to account for such modifications in perovskite-type synthesized materials, a more general formula was adapted in literature:  $A_{1-x}A'_{1-x}B_{1-x}B'_{1-x}O_{3\pm\delta}$ , where the A' and B' symbols represent the possible additions of more than one cation in the structure, as well as its stoichiometric values. The  $\pm\delta$  symbol in the oxide, for instance, represents the excess oxygen necessary to accommodate the formed structures. Examples of perovskites with different formulations are:  $Sr_{0.85}Ce_{0.15}FeO_{3-\delta}$ , also known as CSF structure, and  $Sr_2FeCuO_6$  (HAMMOUDA, et al., 2019; COELHO, et al., 2022).

There are many advantages on the addition of different elements in the sites A and B, such as catalytic power, magnetoresistance, recycle ability, superconductivity, higher dielectric properties, and durability.

As such, many elements may be applied in the synthesis of perovskite materials. Virtually, all cations in the periodic table may be utilized in this structure. In that sense, however, some elements might present higher ability depending on the type of application they are submitted to, and not limited to contaminated water treatment. Perovskites might be applied to many industries, such as the fabrication of alloys, semiconductors, catalysts for industrial processes, thermal-resistant compounds, and others (LI, et al., 2012; ROJAS-CERVANTES, et al., 2019).

Hence, in relation to perovskites application in dark catalysis, some elements might show better performance than others. However, studies regarding the application of perovskites in the remediation of contaminated waters is yet quite limited, even though commercial interest and scientific data have grown significantly in the last years. The next sections present

perovskite-type and perovskites based on three main elements in the degradation of organic contaminants, which are: Iron, Titanium and Lanthanum.

#### *2.2.1.1 Iron (Fe) based catalysts*

Iron oxides are widely known for several properties, such as ferroelectricity, magnetism, electrical conductivity, ease of manipulation and production, availability, and low toxicity. In this context, iron-based perovskites are an interesting and versatile material for application in treatments for environmental remediation (HEIDINGER, et al., 2019; WU, et al., 2019; WANG, et al., 2021).

Several studies have reported and utilized iron-based perovskites for the degradation of different organic contaminants. In Luo, et al., 2010's work, BiFeO<sub>3</sub> was synthesized and utilized for the degradation of RhB, phenol and MB, in a Fenton-like process in an aqueous solution, that is, with the addition of H<sub>2</sub>O<sub>2</sub> as activation reagent, in dark ambient conditions. The concentration of catalyst utilized was of 0.5 g/L, and contaminant concentration in solution was 4.79 g/L. H<sub>2</sub>O<sub>2</sub> for instance was utilized in a concentration of 10 mM. Degradation results were reported as 95.2% reduction in contaminants concentration in 90 min.

LaFeO<sub>3</sub>, for instance, was synthesized and applied on the treatment of several herbicides and pharmaceutical compounds, in Nie, et al., 2015's work. The catalyst concentration was of 1.4 g/L, and the contaminant solution of 3 mg/L. H<sub>2</sub>O<sub>2</sub> concentration, for instance, was of 23mM. The reported results indicated a 100% reduction in SMX's concentration in 2h, at pH 6.5.

Another work (RUSEVOVA, et al., 2014) also utilizing LaFeO<sub>3</sub> verified the catalytic activity and consequent degradation of Phenol and MTBE in an aqueous solution. As such, catalyst concentration was tested in a range of 0.01 to 1g/L, and Phenol and MTBE concentrations, were 25 mg/L and 50 mg/L, respectively. This work also applied H<sub>2</sub>O<sub>2</sub> as the activation reagent, on a concentration of 88 mM. Phenol was reduced by 95% after 6h, and 80% for MTBE, also in 6 h.

Although studies on iron-based perovskites in Fenton-like processes, or with irradiation sources as activation reagents provide relevant results, dark catalysis studies utilizing iron-based perovskites with no activation reagent are limited.



### 2.2.1.2 Titanium (Ti)-based catalysts

Titanium oxide ( $\text{TiO}_2$ ) has been widely used as a powerful oxidant for the degradation of organic contaminants. Titanium has unique properties that allow the synthesis of stable structure, and most importantly, its photocatalytic performance, due to a strong oxidizing power, chemical stability, and cost-effectiveness. However, the use of Titanium oxides in photocatalysis is limited by its large bandgap ( $E_g = 3.2 \text{ eV}$ ), which narrows its application with other sources of irradiation other than UV, since sunlight is composed by only 4% UV light.

Nevertheless, studies using Titanium-based perovskites provided promising results in the degradation of organic contaminants (KUMAR, et al., 2017; WEI, et al., 2021).

In the work of Wang, et al., 2020, a  $\text{SrTiO}_3$  perovskite was synthesized and applied on the degradation of Rhodamine B in an aqueous solution, at a concentration of 5 mg/L. In order to increase the catalyst activity, a doping process was performed, adding Eu in the site A of the perovskite, resulting the doped formula  $\text{Sr}_{0.92}\text{Eu}_{0.08}\text{TiO}_3$ . The catalyst dose was of 0.25 g/L, at pH 7, and temperature of 25 °C. The activation reagent was a Xenon lamp of 300W. The reported results showed a reduction of 95% of the contaminants concentration in 4 hours, using the doped perovskite. The original STO perovskite, however, induced a reported reduction of approximately 36% in RhB concentration in the same period.

A similar methodology was applied by Van-Quoc Truong, et al., 2019, in which the same STO perovskite was tested, however, the sites B and X were replaced and doped by Vanadium and Molybdenum, resulting in the synthesized formula  $\text{SrTi}_{0.9}\text{Mo}_{0.05}\text{V}_{0.05}$ , for the degradation of 10 mg/L solution of Methylene blue. The concentration of the catalyst was 0.5 g/L, at pH 7 and temperature of 31°C. The irradiation source was a compact light in the visible spectrum. Results indicated a 91.5% removal for the doped structure, and 59.9% for the original STO perovskite.

### 2.2.1.3 Lanthanum (La)-based catalysts

Lanthanum oxides have been applied in many forms in electrochemical processes in the last decades, especially those related with Oxygen Reduction Reactions (ORR), due to their unique properties, and particularly promising uses due to the high abundance of lanthanum on Earth, making them candidates for further large-scale application. Several lanthanum perovskites can be formulated by varying the transition metal cation, which, consequently, can impact their catalytic performance (ZHU, et al., 2015; WEI, et al., 2021; DIAS, et al. 2022).

Naturally, lanthanum-based perovskites are on the forefront of many industrial applications and among the most interesting materials in heterogenous catalysis processes.

In Zhang, et al., 2012 work, a  $\text{LaTiCuO}_3$  perovskite was synthesized and tested for the degradation of Rhodamine B, in a concentration of 4.79 g/L. The activation reagent was a solution of 10 mM of  $\text{H}_2\text{O}_2$ , and the concentration of the catalyst was 0.5 g/L. These experiments resulted in 95% reduction in the contaminant of contaminant after 90 minutes, as well as 90% TOC removal in 2 h.

Another interesting work, from Huang, et al., 2020, tested a  $\text{LaFeO}_3$  perovskite structure, however doped in the A site, with the element Bi, resulting in the doped synthesized perovskite  $\text{La}_{0.93}\text{Bi}_{0.07}\text{FeO}_3$  with a band gap of 1.77 eV. This perovskite was tested on the degradation of 2,4-dichlorophenol at a concentration of 10 mg/L. The catalyst dosage was of 2.5 g/L, at pH 7 and temperature 25°C. The activation methodology was photocatalysis, with a 150W Xe lamp. The degradation results showed a reduction of 61% of the phenolic pollutant using the Bi-doped perovskite, and 28% with the original perovskite in 120 minutes.

Moreover, according to Zhou et al. (2019), a  $\text{LaNiO}_3$  perovskite was studied for the degradation of 20 mg/L solution of Tetracycline. The methodology used involved the  $\text{g-C}_3\text{N}_4$  as the support coupled with the target perovskite  $\text{LaNiO}_3$ , in order to increase catalytic activity. The respective bang gaps of each perovskite were 2.68 for the supported catalyst, and 1.89 for the original LNO. The catalyst's dosage was 0.2 g/L, and the irradiation source was a 300 W Xe lamp.

The observed results indicated a reduction of 96% in the contaminant's concentration with the supported perovskite under 300 minutes of light irradiation. The pure LNO perovskite showed a degradation of approximately 32%.

Lastly, another interesting work from Zhang, et al., 2012, in which  $\text{La}_2\text{NiO}_4$  was applied on the degradation of three pollutants: 4-chlorophenol, phenol and Methyl orange. The catalyst concentration was 1.5 g/L, and the removal process was performed in dark conditions at near room temperature and atmospheric pressure. In relation to the process kinetics, it was proposed that the formed ROS were described as  $\text{OH}^-$  and  $\text{O}_2^-$ , as well as the reaction mechanism was Surface Electron Transfer (SET). The results indicated 95% total removal of all contaminants in a period of 12 hours.

Thus, based on the data verified by the papers above discussed, it appears that lanthanum-based perovskites may be effective formulations for the degradation of organic

contaminants and pollutants, even in dark and room temperature and atmospheric pressure conditions.

### 2.3 SYNTHESIS METHOD

Several methods have been employed as complexation routes and preparation procedures for the synthesis of perovskite-type materials. The main methods verified in the literature are usually Hydrothermal, Microwave, Solvothermal, Reverse Microemulsion, Surface-ion adsorption, Dry-Wet Composition, Electrospinning, and Sol-Gel (ROJAS-CERVANTES, et al., 2019).

Among these, however, the Sol-Gel method with EDTA-citrate as complexation reagents has been reported as one of the most efficient synthesis techniques, due to its advantages, such as inexpensive chemical precursors and simple steps. This method, also known as Pechini's method, is based on the preparation of an amorphous gel composed by the intended metallic salts, addition of EDTA, solution dehydration (90°C), and further calcination at temperatures as high as 1000 °C (MAJID, et al., 2015; JAYANTHI, et al., 2022).

In this process, EDTA or Ethylenediaminetetraacetic acid acts as a chelating agent in the segregation of the metallic components. Essentially, the mechanism involves the complexation of metal ions into EDTA or citric acid, followed by the evaporation of water and thermal decomposition of the formed gel in cycles with temperatures ranging from 500°C to 1000°C, resulting in a calcinated material and the perovskite phase.

After these processes, a non-porous coarse brownish powder, with irregular shape and wide particle size distribution, and low specific surface areas is obtained. By that, the perovskite-type structure is complete and ready for utilization depending on the requirements of the intended application (MAJID, et al., 2015; JAYANTHI, et al., 2022).

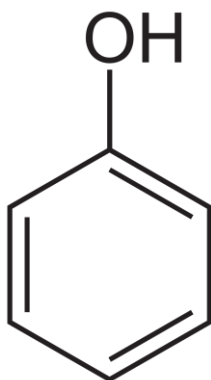
### 2.4 TARGET CONTAMINANT

In this study, Phenol was chosen as a model chemical contaminant for the assessment of the catalytic capacity of metal oxide perovskites in the degradation of these compounds. The selected compound is highly harmful to the environment. Thus, a detailed approach of the properties, applications, as well as the negative impacts reported in the literature will be addressed below.

### 2.4.1 Phenol

Phenol is primarily a natural substance produced by plants, animals, and microorganisms, and also a manufactured chemical. The latter form is a colorless-to-white or light-pink crystalline solid in its pure form and in ambient conditions. It's volatile, with a distinct sweet-tart odor. It is an aromatic hydrocarbon composed by the formula  $C_6H_6O$ , or  $C_6H_5OH$  (CHEN, et al., 2016; AIZAT, et al., 2018). Its structure is shown in the Figure 3.

Figure 3. Phenol molecule. Modified from GUO, et al., 2020.



Phenol is the precursor chemical molecule of several other organic chemicals, used in many industries, especially in chemical engineering with the production of plastics, but also epoxies, resins, nylon, solvents, and pharmaceuticals, making it an important industrial commodity. Its molecule consists of a phenyl group ( $-C_6H_5$ ) bonded to a hydroxyl group ( $-OH$ ) (CHEN, et al., 2016; GUO, et al., 2020).

Among these derivatives, several pollutants share phenol molecules as building blocks of their structure, often paired with halogens. Some of these are: 2-Chlorophenol, 4-Chlorophenol, and bisphenols. Long term exposure to phenol and phenolic pollutants has been associated with cancer, cardiovascular diseases, and illnesses of the respiratory tract. Additionally, ingestion of such chemicals may lead to several gastrointestinal damages and illnesses, as well as organs malfunction and death (LI, et al., 2012).

Phenol is often found in the environment through contaminated waters, such as surface, groundwater, or wastewater. It is highly soluble and contaminated industrial effluents are the main source of manufactured phenol ingress in such environmental compartments. It can be rapidly degraded in air through gas-phase hydroxyl radical reaction, with a half-life estimated in 14.6 hours, but it is considered a persistent chemical in water. Half-lives for

biodegradation range from <1 day in samples of lake water to 9 days in estuarine water; a typical half-life for photooxidation by photochemically produced peroxy radicals is approximately 19 hours. In water, neither volatilization nor sorption to sediments and suspended particulates are expected to be important transport mechanisms (MOHAMMADI, et al., 2015; GUO, et al., 2020).

Although phenol does not absorb light at wavelengths >290 nm, phenols react rapidly to sunlit natural water via an indirect reaction with photochemically produced hydroxyl radicals and peroxy radicals; typical half-lives for hydroxyl and peroxy radical reactions are on the order of 100 and 19.2 hours of sunlight, respectively (MILL, et al., 1985; CANONICA, et al., 1995). These reactions require dissolved natural organic materials that function as photosensitizers (CANONICA, et al., 1995). The estimated half-life for the reaction of phenol with photochemically produced singlet oxygen in sunlit surface waters contaminated by humic substances is 83 days (MOHAMMADI, et al. 2015).

Considering such aspects on phenol presence on the environment, it is imperative that strategies for the efficient removal of phenol or its related compounds from contaminated waters are developed and addressed within the context of scientific research.

### **3 MATERIAL AND METHODS**

This chapter presents the chemical reagents, equipment and procedures used and performed on the synthesis of catalysts and its removal from contaminated waters in dark conditions. The experiments were carried out at the Laboratório de Transferência de Massa – LABMASSA – Departamento de Engenharia Química e de Alimentos da Universidade Federal de Santa Catarina (UFSC).

#### **3.1 CHEMICAL REAGENTS**

In the present work, perovskite-type catalysts of different formulations were synthesized via the Sol-Gel Method with the complexation route of EDTA-citrate, and slight modifications in the performed procedures. The Table 1 below presents the chemical precursors utilized, as well as their technical specifications.

Table 1. Chemical Products Utilized in the Synthesis and its Specifications.

<b>Chemical Name</b>	<b>Formula</b>	<b>Brand</b>	<b>Purity (%)</b>	<b>Solubility (g/mL)</b>	<b>Use</b>
Lanthanum Nitrate Hexahydrate	La (NO <sub>3</sub> ) <sub>3</sub> .6H <sub>2</sub> O	Metaquímica	>99.0	1.4	Metallic Compound
Iron Nitrate Nonahydrate	Fe (NO <sub>3</sub> ) <sub>3</sub> .9H <sub>2</sub> O	Dinâmica	>99.0	2.67	Metallic Compound
Titanium Dioxide	TiO <sub>2</sub>	Dinâmica	>99.0	0.94	Metallic Compound
Citric Acid	C <sub>6</sub> H <sub>8</sub> O <sub>7</sub> .H <sub>2</sub> O	Neon	>99.5	0.88	Chelating Agent
EDTA	C <sub>10</sub> H <sub>16</sub> N <sub>2</sub> O <sub>8</sub>	Neon	>99.0	-	Chelating Agent
Ammonium Hydroxide 35%	NH <sub>4</sub> OH	Dinâmica	>97.5%	-	pH Buffer

Source: Author.

In that sense, a common molecule of several organic pollutants was studied in this work. The Table 2 below presents the technical specifications for Phenol.

Table 2. Target Pollutant Specifications.

<b>Chemical Name</b>	<b>Formula</b>	<b>Brand</b>	<b>Purity (%)</b>	<b>Solubility (g/mL)</b>	<b>Use</b>
Phenol	C <sub>6</sub> H <sub>5</sub> OH	Neon	>99.0	0.08	Target Pollutant

Source: Author.

As previously mentioned, the studied catalysts were prepared by the Sol-Gel method with EDTA-citrate complexation route. This method is based on the preparation of an amorphous gel composed by the intended metallic salts, addition of EDTA, solution

dehydration (90°C), and further calcination at temperatures as high as 1000 °C (MAJID, et al., 2015; JAYANTHI, et al., 2022).

In this process, EDTA and citric acid act as chelating agents in the segregation of the metallic components. Essentially, the mechanism involves the complexation of metal ions with EDTA and citric acid, followed by the evaporation of water and thermal decomposition of the formed gel in cycles with temperatures ranging from 500°C to 1000°C, resulting in a calcinated material and the perovskite phase. A non-porous coarse brownish powder, with irregular shape and wide particle size distribution, and low specific surface areas is obtained. By that, the perovskite-type structure is complete and ready for utilization depending on the requirements of the intended application (MAJID, et al., 2015; JAYANTHI, et al., 2022).

The utilized molar ratios of the precursor chemicals, that is, the metal ions, citric acid, EDTA and ammonium hydroxide were 1:2:1.1:10, respectively. After the quantity's definition of the required chemicals and weighing, EDTA was mixed into 35% solution of ammonium hydroxide prepared at room temperature and constant stirring on a magnetic stirrer until completely homogenized. Subsequently, the weighted quantities of the metallic ions were poured into a separate solution with 80 mL of deionized water with constant stirring in order to dissolve all the metallic compounds in the solution. Following the dissolution of the metallic ions, the citric acid was added to the solution, and the prepared alkaline EDTA solution was slowly added and mixed with the metallic-citrate solution. After these procedures at constant stirring, the solution was adjusted for pH 7, by the addition of droplets of concentrated ammonium hydroxide controlled by a Pasteur pipette (eye dropper), and the monitoring of pH by a pH meter.

The solution was then heated to 90°C for approximately 3 h, until an amorphous gel was formed, and the water evaporated from the solution. Furtherly, the obtained gel-like mixture was calcined in a muffle oven at 450 °C for 8 h using a heating and cooling rate of 5 °C min<sup>-1</sup>, as the first calcination step. After this process, the resulting crystallized material was grinded using mortar and pistil, and then sieved through a 325 mesh (44 µm) sieve, in order to deagglomerate coarse particles. Finally, a last calcination step was performed at 1000 °C for 8h and at heating and cooling rate of 5 °C min<sup>-1</sup>.

However, the catalyst LaNiFeO<sub>3</sub> was subjected to three different final calcination steps, with 750 °C, 800 °C and 1000 °C as the respective utilized temperatures. The goal of this

modification was to verify the changes in the obtained catalysts structures in order to identify morphological differences that could result in different catalytic capacities.

It is also important to highlight that all synthesized catalysts considered the general formula  $A_{1-x}A'_{1-x}B_{1-x}B'_{1-x}O_{3\pm\delta}$ , with no excess. Hence, the stoichiometric ratio of the metals utilized in both sites (A, B and O) was 1:1:3.

## 3.2 CHARACTERIZATION TECHNIQUES

### 3.2.1 Scanning Electron Microscopy (SEM) and Energy Dispersive X-Ray Spectroscopy (EDS)

Scanning Electron Microscopy (SEM) and Energy Dispersive X-Ray Spectroscopy (EDS) techniques were utilized for the verification of the surface morphologies of the synthesized catalysts, as well as for the elemental mapping of the ions present in the sample. The tests were performed with a JEOL scanning electron microscope (model JSM- 6390 LV) equipped with a system for performing simultaneous chemical analysis using energy scattering X-ray spectroscopy (EDX). The preparation of the materials for the analysis consisted of fixing the powdered samples to a metal support (*stub*) with carbon tape. No coating element was utilized. The analyses were performed at the Federal University of Santa Catarina with the collaboration of the team of the Central Laboratory of Electron Microscopy (LCME).

### 3.2.2 Surface Area (BET)

Brunauer-Emmett-Teller (BET) analysis was also utilized for the characterization aspects of the surface area of the catalysts. In BET's analysis, multi-point measurements are taken through gas adsorption into the pores of the catalyst, hence it is possible to classify the different measurements into microporous, mesoporous, or microporous (LI, et al., 2012). The performed analysis consisted of pre-treatment of the samples of outgas at 300°C and, subsequently, submitted to adsorption in liquid nitrogen in an automatic physisorption equipment of the brand Quantachrome, model Autosorb-1. The analyses were carried out at the Universidade Federal de Santa Catarina (UFSC), with the collaboration of the Centro de Análises do Departamento de Engenharia Química e de Alimentos (CAEQA).

### 3.2.3 Zeta Potential (ZP)

Zeta-Potential analysis was also employed to investigate the characteristics of the surface of the studied materials. Zeta-Potential is a physical property of suspended materials as



it determines the stability of colloidal suspensions. In this method, it is possible to verify how the surface of the catalysts are charged, as well as its potential to maintain colloidal suspensions (MALVERN, 2015). The tests were performed at a Zetasizer Nano ZS Malvern, in a temperature of 25°C, an attenuation coefficient of 0.131 and a refraction index of 2.6044. The experiments were performed at the Universidade Federal de Santa Catarina, with the collaboration of the Laboratório Interdisciplinar de Desenvolvimento de Nanoestruturas (LINDEN).

### **3.2.4 X-Ray Diffraction (XRD)**

X-Ray Diffraction (XRD) analyzes were performed in the synthesized catalysts. This characterization technique provides information on the structure and the preferential crystal orientation of the catalyst, as well as other parameters such as chemical composition and grain size. For this analysis, the samples were irradiated with incident X-Rays using  $K\alpha$  radiation at  $\lambda = 1.5418 \text{ \AA}$ , generated with 45 kV, 40 mA, in which the resulting intensities and scattering angles of the reflected rays in the surface indicate the above-mentioned characteristics of the studied material (AIZAT, et al. 2018). The analyzes were made by a MiniFlex 600 DRX Rigaku. The parameters of the analyzes utilized a step size of  $0.02985^\circ$ , an angular range of 5 to  $90^\circ$  ( $2\theta$ ), and a screening speed of  $15^\circ$ . The tests were performed at the Universidade Federal de Santa Catarina, with the collaboration of the Laboratório Interdisciplinar de Desenvolvimento de Nanoestruturas (LINDEN).

### **3.2.5 Fourier Transform Infrared Spectroscopy (FTIR)**

The Fourier Transform Infrared Spectroscopy provides information on the absorbance of Infrared radiation in the studied materials. The resulting spectrum gives insights of chemical bonds, and the understanding of the behavior and properties of the catalysts. Therefore, FTIR analyzes were carried out in the synthesized materials. For this work, the analyzes were performed in the spectral range of 4000 to  $400 \text{ cm}^{-1}$ , resolution of  $4 \text{ cm}^{-1}$ , and 0.1% Potassium Bromide (KBr) tablets mixed into the samples. The equipment utilized was an infrared spectrophotometer model Cary 660 (Agilent Technologies). The analyses were made at the Universidade Federal de Santa Catarina (UFSC), with the collaboration of the Centro de Análises do Departamento de Engenharia Química e de Alimentos (CAEQA) da UFSC.

### 3.3 ANALYTICAL TECHNIQUES

#### 3.3.1 High Performance Liquid Chromatography (HPLC)

In order to investigate the degradation of the target contaminants, as well as the formation of intermediate compounds, High Performance Liquid Chromatography analyzes were performed in the samples properly retrieved from the degradation experiments. The analyzes were performed utilizing a C18 5 $\mu$ m (150 x 4.6 mm) reverse phase column at a Shimadzu SPD-10A HPLC equipment. The mobile phase for Phenol was a mixture of acetonitrile, ultrapure water and trifluoroacetic acid (TFA), in the respective ratio 30:70:1 (v/v). The flow rate or the elution rate was 0.5 mL/min, the retention time was 10 min, and the volume of the samples was 20  $\mu$ L. The wavelength utilized for Phenol was 270 nm, and the temperature of the analyses was 25C. The analyses were performed at the Laboratório de Transferência de Massa (LABMASSA) of the Universidade Federal de Santa Catarina.

### 3.4 EVALUATION OF CATALYTIC ACTIVITY

#### 3.4.1 Degradation Kinetics

The synthesized catalysts were subjected to degradation experiments with the target contaminant Phenol for the assessment of their catalytic capacity in degrading the contaminant. These experiments were performed with different setups and parameters, especially related to temperature and degradation time, as shown below in Table 3.

Table 3. Degradation Experiment Parameters.

Catalyst	Catalyst Mass (g)	Contaminant Concentration (mg/L)	Temperature (°C)	Time (min)	Sampling Interval (min)
<b>Test 01</b>					
LaTiO <sub>3</sub>	0.3	20	25	180	30
LaFeO <sub>3</sub>	0.3	20	25	180	30
<b>Test 02</b>					
LaTiO <sub>3</sub>	0.3	20	25	720	30
LaFeO <sub>3</sub>	0.3	20	25	720	30

Catalyst	Catalyst Mass (g)	Contaminant Concentration (mg/L)	Temperature (°C)	Time (min)	Sampling Interval (min)
<b>Test 03</b>					
<sup>1</sup> LaNiFeO <sub>3</sub>	0.3	20	25	180	30
<sup>2</sup> LaNiFeO <sub>3</sub>	0.3	20	25	180	30
<sup>3</sup> LaNiFeO <sub>3</sub>	0.3	20	25	180	30
<b>Test 04</b>					
<sup>1</sup> LaNiFeO <sub>3</sub>	0.3	20	60	180	30
<sup>2</sup> LaNiFeO <sub>3</sub>	0.3	20	60	180	30
<sup>3</sup> LaNiFeO <sub>3</sub>	0.3	20	60	180	30

Source: Author. Notes: <sup>1</sup>Synthesis T°C = 700; <sup>2</sup>Synthesis T°C = 850; <sup>3</sup>Synthesis T°C = 1000;

These tests intended to provide different outcomes for the degradation of the target contaminant. To ensure the distribution of the catalyst, the test solution was kept under magnetic agitation throughout the entire degradation processes. The retrieved aliquots (2 mL) were sampled from the reaction suspension and filtered in a 0.45 µm (*millipore*) syringe filter at the pre-fixed intervals shown above.

## 4 RESULTS AND DISCUSSION

The following sections in this chapter will present the observed results and main findings of the experiments carried out in this work and discuss such results with recent scientific papers in the literature.

This assessment will englobe the synthesis methods employed on the preparation of the catalysts, characterization techniques, and the analytical data obtained from the degradation kinetics of the target contaminant, as well as to provide insights into the mechanisms of degradation.

Ultimately, the discussion below envisions to provide a critical view on the application of perovskite-type catalysts in dark conditions as a relevant and cost-effective type of treatment for emerging contaminants, not depending in chemical reagents activation or light irradiation.

### 4.1 LaFeO<sub>3</sub> PEROVSKITE-TYPE LANTHANUM BASED CATALYST

As previously presented, three catalysts were chosen as promising materials on the degradation of the target contaminant, Phenol. Among these, LaFeO<sub>3</sub> was the first synthesized catalyst of this work. Lanthanum-Iron oxide catalysts (LFO) are well-known oxides in literature, and they have been applied in a range of treatment techniques in heterogenous catalysis due to its unique electronic properties and cost-effectiveness, making it a promising catalyst for a wide range of applications (HUMAYUN, et al., 2016; WEI, et al., 2021).

The inclusion of Iron and Lanthanum as mixed oxides are due to their unique aspects and properties, such as a stable chemical structure, ease of operation, synthesis process, and oxidation potential. Lanthanum has an Eg of 1.89-2.71 eV and Iron of 2.0 eV. Besides these properties, the inclusion of Iron in such formulations considerably reduces costs since it is a highly available metal (RUSEVOVA, et al., 2014; NIE, et al., 2015).

As such, several studies have demonstrated the ability of LFO catalysts in the degradation of several organic contaminants (ROJAS-CERVANTES, et al., 2019; WANG, et al., 2021). However, not many works focused on the utilization of LFO catalysts in dark catalysis, that is, in the absence of any type of light irradiation.

Hence, the following items will delve into the results observed from the synthesis of the LFO catalyst to its degradation capacity in relation to the target contaminant, phenol.

#### 4.1.1 Catalyst Synthesis

The method employed for the synthesis of the LaFeO<sub>3</sub> catalyst was carried out as presented in the Section 3, known as Sol-Gel with EDTA-Citrate route. The masses and volumes of the utilized compounds are shown in the Table 4, below.

Table 4. Chemical Reagents Quantities for LaFeO<sub>3</sub> Synthesis Process.

Chemical Name	Formula	Mass (g)	Volume (mL)
Lanthanum Nitrate Hexahydrate	La (NO <sub>3</sub> ) <sub>3</sub> .6H <sub>2</sub> O	5.29	
Iron Nitrate Nonahydrate	Fe (NO <sub>3</sub> ) <sub>3</sub> .9H <sub>2</sub> O	4.63	-
Citric Acid	C <sub>6</sub> H <sub>8</sub> O <sub>7</sub> .H <sub>2</sub> O	10.28	-
EDTA	C <sub>10</sub> H <sub>16</sub> N <sub>2</sub> O <sub>8</sub>	7.89	-
Ammonium Hydroxide 35%	NH <sub>4</sub> OH	-	9.84

Source: Author.

The calculation of the required mass and volume for the preparation of approximately 3 grams of LaFeO<sub>3</sub> perovskite was based on the molecular weight of the metallic salts and their respective solubility, and purity grade. After obtaining the mass of metallic salts necessary for the formulation, the same procedure was utilized to calculate the requirements for the reagents involved in the process, which are citric acid, EDTA and Ammonium Hydroxide 35%. All measurements were made considering the ratio 1:2:1.1:10, for the metallic salts, citric acid, EDTA and ammonium hydroxide, respectively.

After the mixing and execution of the synthesis procedures, the resulting mass of the calcined catalyst was verified as 2.14 g.

The Figure 4, below, showcases a mosaic of pictures obtained during the process of synthesis.

Figure 4. Synthesis Steps of LaFeO<sub>3</sub> Perovskite.



Source: Author.

Many papers have described perovskite-type materials as greyish, black, or brownish materials after calcination, depending on the temperatures utilized. Wu, et al., 2019, proposed a different synthesis procedure based on the Sol-Gel method as well, with an overnight drying period at 105°C, and only one step of calcination at 700°C for 5 h. This methodology however did not result in the formation of the calcined structure that differentiates and highlights the perovskite-like catalysts. Yet, it yielded a material with relevant amount of humidity after the calcination step.

For the synthesized LFO catalyst, however, as shown in Figure 4, a totally dried up material was obtained after the calcination steps of 480°C and 1000°C, for 8 h at a heating and cooling rate of 5 °C.min<sup>-1</sup>. The use of Iron salts has probably influenced the brownish and ferruginous coloring of the acquired catalysts.

Thus, after calcination, the obtained samples of the LFO catalyst were grinded and sifted in order to break and separate larger particles conglomerates, successfully increasing grains distribution and its superficial area.

#### 4.1.2 Degradation Kinetics and Catalytic Activity

The following acquired data demonstrates the degradation rates obtained while working with LaFeO<sub>3</sub> catalyst in two different degradation events.

As aforementioned, the use of a Lanthanum-Iron catalyst was based on the capacity of Iron and Lanthanum oxides on the degradation of organic contaminants. Hence, the performed experiments meant to verify and evaluate such abilities in dark conditions, with no chemical activation agents and no light irradiation. However, in order to testify the potential enhancement

of the catalytic performance of LFO catalyst, heating and extended periods of degradation were also verified for comparison and discussion.

#### *4.1.2.1 Catalytic Performance*

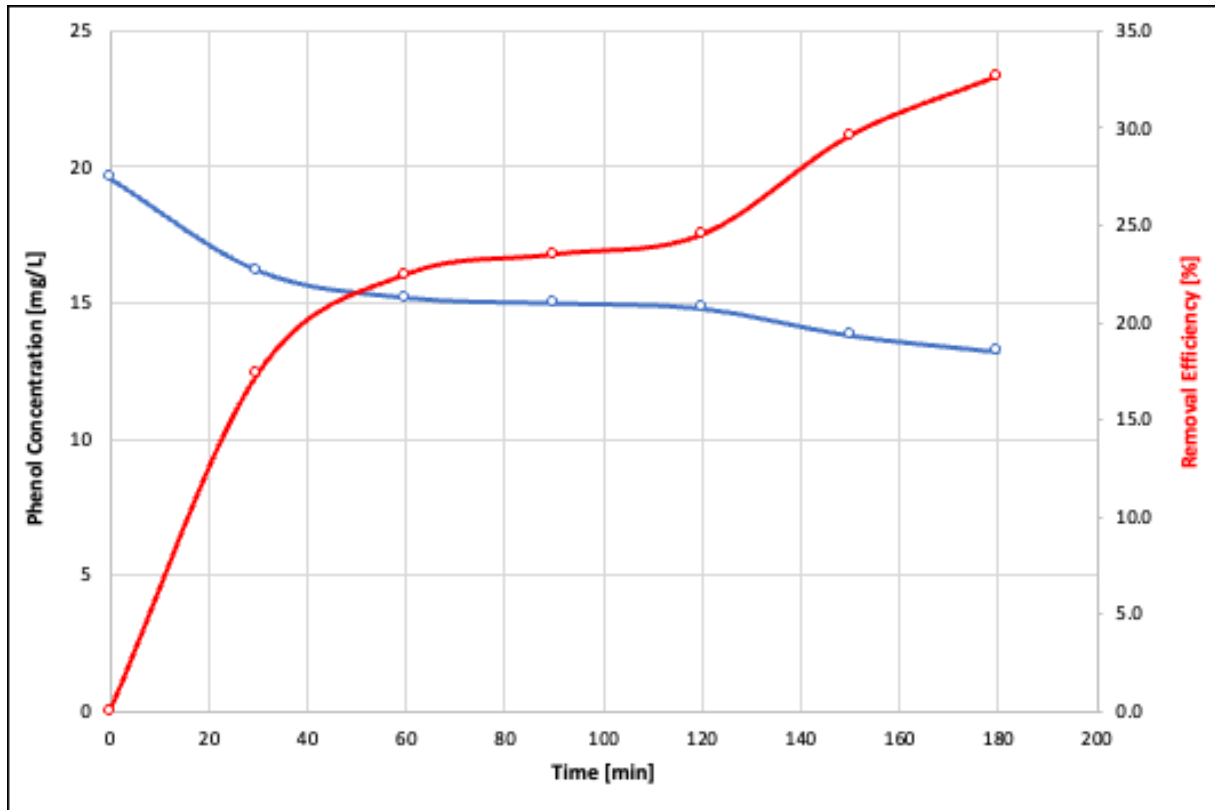
The first degradation experiment made with the LFO perovskite-type catalyst involved the 0.3 g of LFO and 20 mg/L of phenol. The reactor was then stirred constantly at room temperature and atmospheric pressure, pH 7, and at the absence of light. The experiment was carried out for 180 min (3h), and samples were taken at 0 min, 30 min, 60 min, 90 min, 120 min, 150 min, and 180 min.

The aliquots of 2 mL from each time slot were acquired using a Pasteur pipette, and then filtered through a 0.22  $\mu\text{m}$  Millipore filter, by the utilization of a 5 mL syringe, in order to separate the content of the reactor from the metallic oxides present in the solution. The remaining volume with the filtered degraded phenolic compounds was then poured into 1.5 mL vials for HPLC analysis.

The analytical method utilized for the verification of the degradation performance of phenol involved parameters often employed for the analysis of the contaminant in the literature. During the analysis, the phenol distinctive peak was observed between 7 and 7.5 min after the start of the screening procedure for each sample.

The Figure 5, below, demonstrates the rate of degradation achieved by the LFO-catalyst in the first experimental conditions tested, obtained from the measurements made during the screening procedures of the samples analyzed for phenol via HPLC.

Figure 5. First Experiment Results for Phenol Degradation Performance by LaFeO<sub>3</sub>.



Source: Author.

The interpretation of the data presented above was based on the Equation 5, which resulted on the likely concentrations obtained for phenol at the analyzed samples.

Equation 5. HPLC Measurements Conversion to Phenol Concentration in mg/L.

$$C1 = \frac{A+1208.8}{20690}$$

Where:

C1 = Contaminant Concentration, in mg/L; and

A = Area (volts).

In this particular test, a 32.8% degradation performance was observed. Such value is considered relevant, and it is backed up by data verified in the literature for the same LFO formulation. As a matter of fact, the works of Rusevova, et al., 2014, and Taran, et al., 2016 found degradation rates of 90% in 6 h and 80% in 2.2 h for phenol, respectively. Although,



such experiments were carried out involving chemical reagents such as  $\text{H}_2\text{O}_2$  and PMS, which can significantly enhance the catalytic activity of perovskites. Hence, considering the experimental conditions in which LFO catalyst was applied, such degradation rate might be promising.

For the second test utilizing  $\text{LaFeO}_3$  perovskite-type catalyst, the experimental conditions were slightly modified in order to verify which changes would be observed in the degradation patterns for phenol.

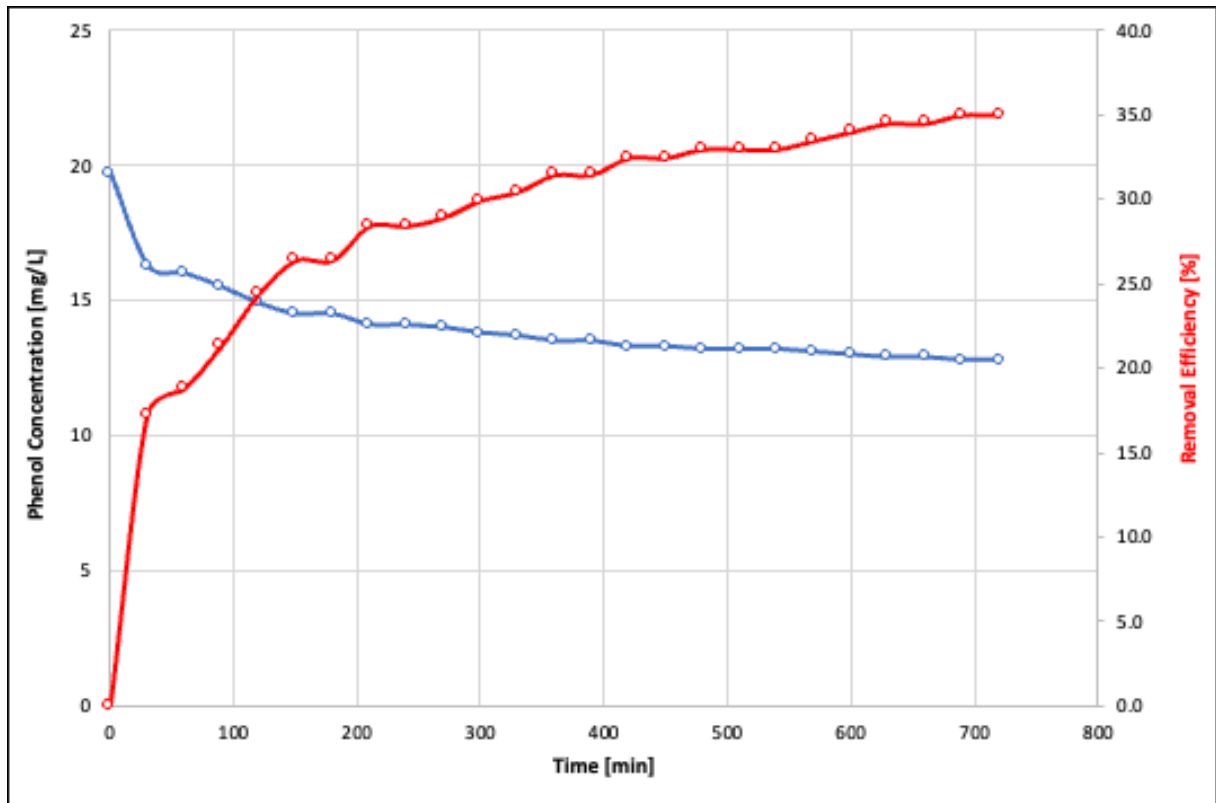
Thus, this test considered the same mass of 0.3g of LFO and 20 mg/L of Phenol. The reactor was then stirred constantly at room temperature and atmospheric pressure, pH 7, and at the absence of light. The experiment was performed during 720 min (12h), instead of 3h, and samples were taken at 0 min and subsequently after 30 minutes until the experiment was concluded at 720 min.

As such, the aliquots of 2 mL from each time slot were acquired using a Pasteur pipette, and then filtered through a 0.22  $\mu\text{m}$  Millipore filter, by the utilization of a 5 mL syringe, in order to separate the content of the reactor from the metallic oxides present in the solution. The remaining volume with the filtered degraded phenolic compounds was then poured into 1.5 mL vials for HPLC analysis.

Applying the same methodology presented in Equation 5, phenol concentrations after degradation were obtained for the second test. The

Figure 6, below, demonstrates the degradation rate for the LFO-catalyst results acquired for the second degradation test of phenol during 12 h.

Figure 6. Second Experiment Results for Phenol Degradation Performance by  $\text{LaFeO}_3$ .



Source: Author.

Based on the data above, a similar pattern was observed when compared to the first experiment, which had a duration of only 3 h. The degradation performance obtained for the second event was verified as 35.1%.

Moreover, it appears that LFO-catalyst has higher degradation rates at the first 30 min of operation. As such, phenol concentrations decreased from 19.6 mg/L at 0 min to 16.2 mg/L at 30 min, representing a reduction of 17.3%. For the second test, virtually the same decrease was observed between 0 and 30 min, resulting in a 17.2% reduction. Additionally, both degradation rates could be described as sixth order polynomials.

Thus, even though the data presented above indicates that LFO-perovskites do possess relevant degradation rates, improvements might be needed to enhance its catalytic activity towards organic contaminants.

## 4.2 LaTiO<sub>3</sub> PEROVSKITE-TYPE LANTHANUM BASED CATALYST

The second catalyst to be synthesized in this work was the formulation LaTiO<sub>3</sub>, which involved the utilization of the precursor elements Lanthanum and Titanium in a perovskite-type structure.

The utilization of TiO<sub>2</sub> is largely reported in the literature for applications on photocatalysis. It has been reported as a powerful oxidant in the treatment of several organic contaminants, as seen on the papers of Wei, et al. 2021, and Wang, et al., 2021.

Due to its unique characteristics, which differentiates it as a low-cost semi-conductor with a band gap of 3.2 eV that is capable of generating several ROS when excited by UV light, the synthesis of a Lanthanum-Titanium perovskite-type (LTO) material might provide useful data for the degradation of organic contaminants in dark conditions. However, these same properties might influence in its ability to degrade contaminants in the dark, since its large band gap can only be excited via UV-lighting (SALAS, et al., 2013; GRABOWSKA, et al., 2016; WEI, et al., 2021).

Moreover, few papers have presented the utilization of Titanium on the degradation of phenolic compounds. Thus, the following items will present the results observed during the synthesis of the LTO-catalyst, as well as its degradation capacity towards the target contaminant, phenol.

### 4.2.1 Catalyst Synthesis

As previously presented, the method utilized for the synthesis of all catalysts was the Sol-Gel method with the application of EDTA-Citrate route. For the LTO-catalyst, the same procedures described in Section 3 were applied.

The Table 5, below, computes the chemical precursors, chemical reagents and complexing agents utilized in the synthesis of LaTiO<sub>3</sub>, as well as its properties and quantities.

Table 5. Chemical Reagents Quantities for Synthesis Process of LaTiO<sub>3</sub>.

Chemical Name	Formula	Mass (g)	Volume (mL)
Lanthanum Nitrate Hexahydrate	La (NO <sub>3</sub> ) <sub>3</sub> .6H <sub>2</sub> O	5.12	
Titanium Oxide	TiO <sub>2</sub>	0.94	-
Citric Acid	C <sub>6</sub> H <sub>8</sub> O <sub>7</sub> .H <sub>2</sub> O	9.95	-

Chemical Name	Formula	Mass (g)	Volume (mL)
EDTA	$C_{10}H_{16}N_2O_8$	7.64	-
Ammonium Hydroxide 35%	$NH_4OH$	-	9.53

Source: Author.

The calculated amount of chemicals utilized resulted in approximately 2.36 grams of  $LaTiO_3$  perovskite after all mixing procedures and calcination steps. The required masses and volumes were adjusted based on the molecular weight of the metallic precursors, solubility, and purity grade. For the LTO-catalyst, the same ratio of 1:2:1.1:10 was utilized for the metallic precursors, citric acid, EDTA and ammonium hydroxide, respectively. The Figure 7, below, depicts a mosaic of pictures obtained during the process of synthesis of  $LaTiO_3$ .

Figure 7. Synthesis Steps of  $LaTiO_3$  Perovskite.



Source: prepared by the author.

As shown above, the synthesis of the LTO-catalyst resulted in a greyish-black fine powder and successful perovskite-type structure, as reported in a few papers (GARCIA-MUNOZ, et al., 2019; and 2020). Following the release of such species, organic molecules in the medium tend to break bonds and form new byproducts.

The white coloring from the mixed metal oxides is due to the color of the titanium oxide, as well as the greyish to black coloring of the powder might also have been influenced by the chemicals utilized.

The procedure applied for the synthesis of  $\text{LaTiO}_3$  involved the evaporation of the water content in the mixture, and subsequently the steps of calcination in which, at first, the samples were calcined in the muffle at  $480\text{ }^\circ\text{C}$ , followed by the last calcination step of  $1000\text{ }^\circ\text{C}$ , for 8 hours at a heating and cooling rate of  $5\text{ }^\circ\text{C min}^{-1}$ . The powder was then refined by a mortar and pestle utensils and, finally, sifted for the retention of conglomerates.

#### **4.2.2 Degradation Kinetics and Catalytic Activity**

The degradation experiments performed utilizing the LTO-catalyst had the same experimental conditions as the one applied to the  $\text{LaFeO}_3$  perovskite. As previously mentioned,  $\text{TiO}_2$  has been largely used as a photocatalyst in several industries, however, few studies reported its utilization in dark catalysis.

Thus, the results obtained for the degradation of Phenol while employing the  $\text{LaTiO}_3$  perovskite in dark conditions are presented and discussed in the following section.

##### *4.2.2.1 Catalytic Performance*

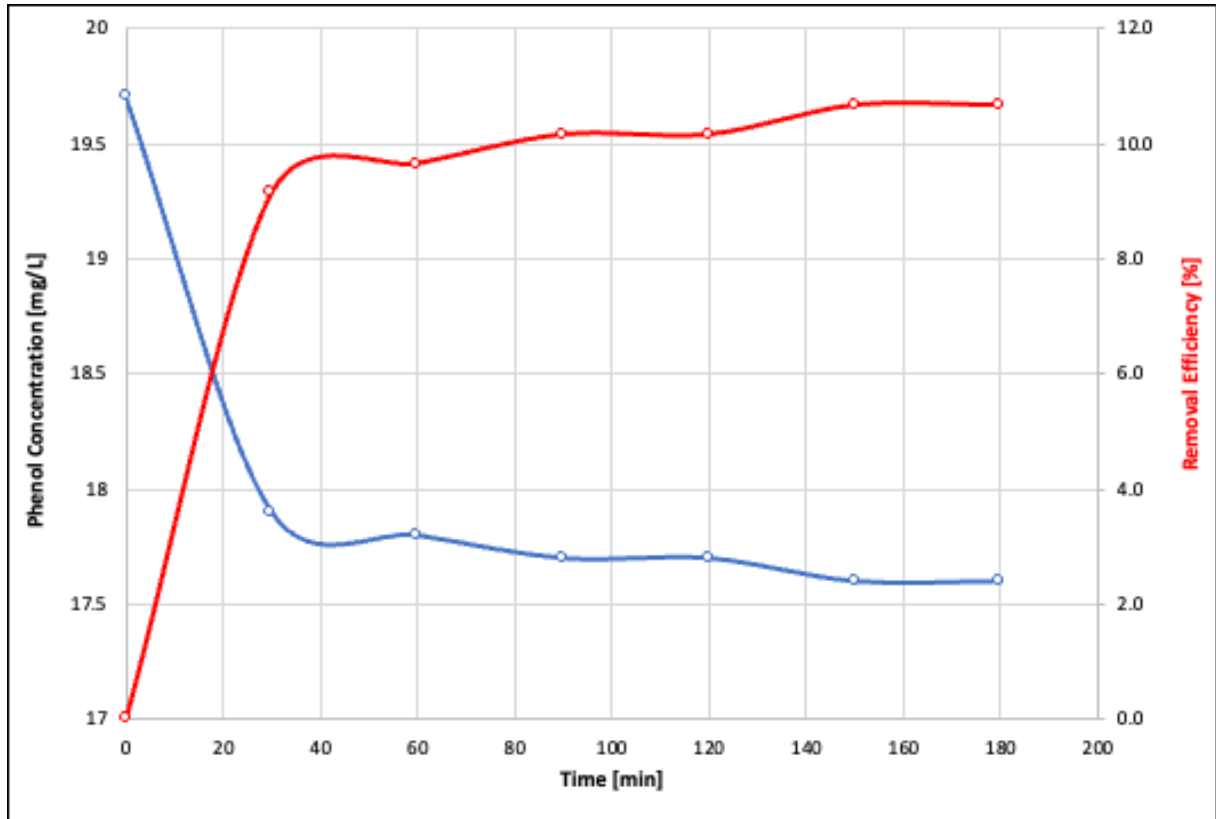
Two different tests were carried out with the LTO-catalyst, which varied the temperature utilized throughout the degradation process.

The first degradation test considered 0.3 g of the LTO-catalyst and approximately 20 mg/L of phenol into a batch reactor. The reactor was then stirred constantly at room temperature and atmospheric pressure, pH 7, and at the absence of light. The experiment was carried out for 180 min (3h), and samples were taken at 0 min, 30 min, 60 min, 90 min, 120 min, 150 min, and 180 min, such as the methodology applied to the  $\text{LaFeO}_3$  catalyst.

Such aliquots from each time slot had 2 mL of the degraded solution and were acquired using a Pasteur pipette, and filtered through a  $0.22\text{ }\mu\text{m}$  Millipore filter, by the utilization of a 5 mL syringe, as part of the sample preparation process for analysis at the utilized HPLC equipment. The filtered samples were poured into 1.5 mL vials.

The Figure 8, below, demonstrates the degradation pattern verified for the first degradation experiment with LTO-catalyst and computes the measurements made for the analytical procedure with the HPLC equipment.

Figure 8. First Experiment Results for Phenol Degradation Performance by  $\text{LaTiO}_3$ .



Source: Author.

The degradation observed for phenol while using the LTO-catalyst was of 10.6%. Such value is below to what is reported in the literature for similar works (HUMAYUN, et al., 2016; NIE, et al., 2019). Although, as previously highlighted in the present work, most of the papers in which Titanium stood as the only oxide for the degradation of organic contaminants also utilized sources of light and/or chemical activators for the enhancement of the catalytic performance.

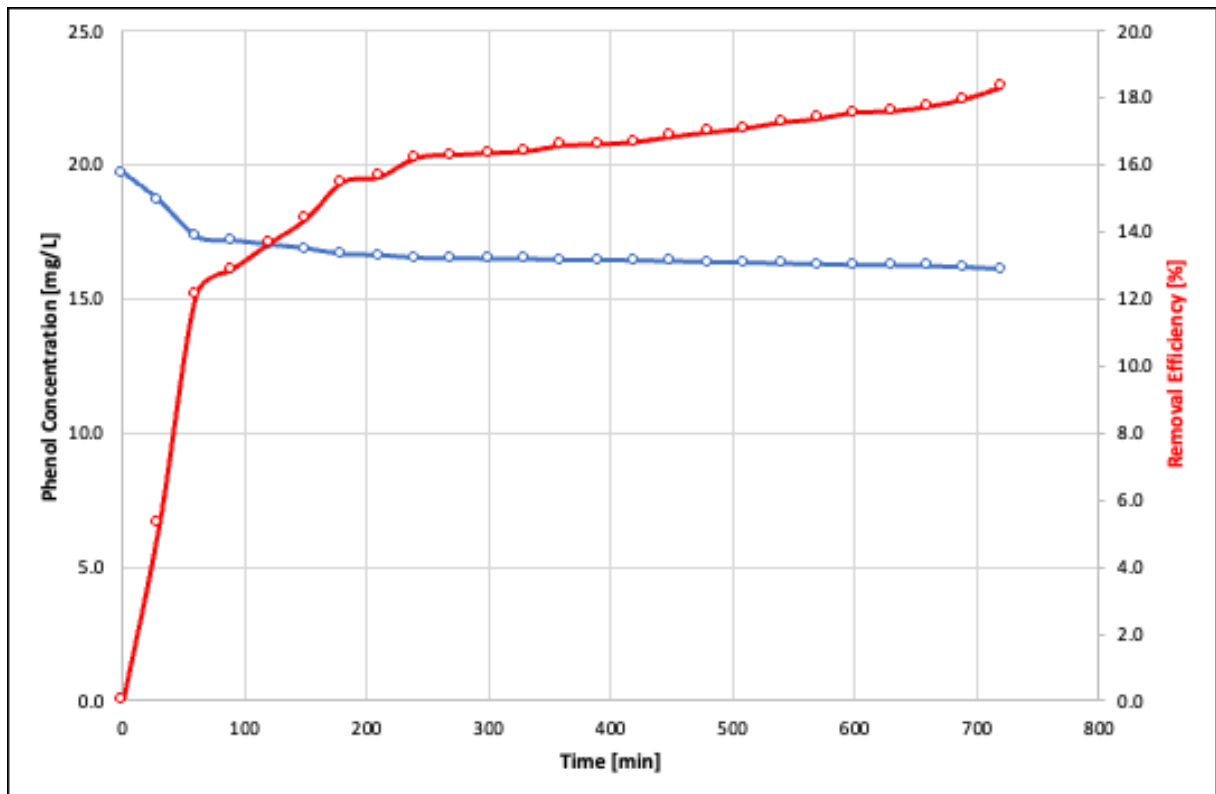
On the second test performed for the LTO-catalyst, the experimental conditions were modified as well in regard to the time in which the degradation experiment was carried out, which was 720 min (12h).

All other experimental parameters however remained the same, with approximately 0.3g of LTO and 20 mg/L of Phenol in the reactor, stirred constantly at room temperature and

atmospheric pressure, pH 7, and at the absence of light. Samples were taken at 0 min and subsequently after 30 minutes until the experiment was concluded at 720 min.

Additionally, the same procedure already elucidated for the preparation of the retrieved aliquots for HPLC analysis was also performed. The Figure 9, below, computes the data acquired from HPLC as well as the conversion of the peak areas to phenol concentration, using Equation 5.

Figure 9. Second Experiment Results for Phenol Degradation Performance by  $\text{LaTiO}_3$



Source: Author.

Considering the data obtained above for the second degradation test with LTO and Phenol, a degradation performance of 18.3% has been verified after 12 h. Such value is still below what has been reported in the literature, however, the dark conditions of the test with no use of any light irradiation or energy source might have inflicted in Titanium's activity towards the target contaminant.

Thus, based on the behavior seen above, it is possible to identify that the LTO perovskite induces greater degradation at the target contaminant during approximately 90 minutes, with a very low performance in the period after such threshold. This may be due to



less ROS being formed after the perovskite particles become saturated from the contaminated solution.

Nevertheless, as previously highlighted in the present work, not many studies have been published investigating the catalytic activity of Titanium perovskites in dark conditions and with no activation agents or light irradiation, therefore the results verified in such experiments may provide evidence in such subject and assist future works with the use of Titanium in perovskites treatment of organic contaminants.

#### 4.3 LaNiFeO<sub>3</sub> PEROVSKITE-TYPE LANTHANUM BASED CATALYST

The Lanthanum-Nickel-Iron perovskite was the third and last formulation to be tested in this work. As previously presented, the study and proposal of such perovskite was based on the literature observed for LaFeO<sub>3</sub> and LaNiO<sub>3</sub> catalysts, which are promising mixed metal oxides for the application in a vast range of techniques on contaminated water treatment.

The results obtained for LaFeO<sub>3</sub> settles a line of evidence for the employment of formulation involving Iron, due to its versatility, availability, and cost-effectiveness on the degradation of organic contaminants.

Nickel oxides, for instance, are also known for its abilities as a catalyst for many types of treatment, as well as its availability, cost-effectiveness and ease of operation, chemical stability, and electrochemical properties. Scientific papers describing the use of LNFO catalysts are very limited. Such metallic oxides are often prepared and tested in separate tests (WU, et al., 2010; LI, et al., 2012; and PALAS, et al., 2018).

Thus, the mixing of such metallic precursors into a new composite capable of enhancing the degradation of the target contaminant in dark conditions has been the subject of research for the next portion of this work. The next sections will provide the results verified on the synthesis, degradation capacity, and characterization of the LNFO catalyst.

##### 4.3.1 Catalyst Synthesis

For the synthesis of the LNFO catalyst, the same Sol-Gel modified methodology was applied. However, the last calcination step involved in the process of synthesis was also modified as part of the investigation on the effect of synthesis and preparation methods on the physical and catalytic properties of perovskites.

Henceforth, three different tests were performed, considering the last calcination step with temperatures of 700 °C, 850 °C and 1000 °C. Such modification also considered reports made in the literature, in which different procedures were applied to the Sol-Gel EDTA-Citrate route method. It is important to note, however, that only the last calcination step on the synthesis of LNFO perovskites was modified in the method, hence all other parameters were performed as presented in Section 3.

The Table 6. Chemical Reagents Quantities for Synthesis Process of LaNiFeO<sub>3</sub>, below, details the quantities utilized for the LNFO-catalyst.

Table 6. Chemical Reagents Quantities for Synthesis Process of LaNiFeO<sub>3</sub>

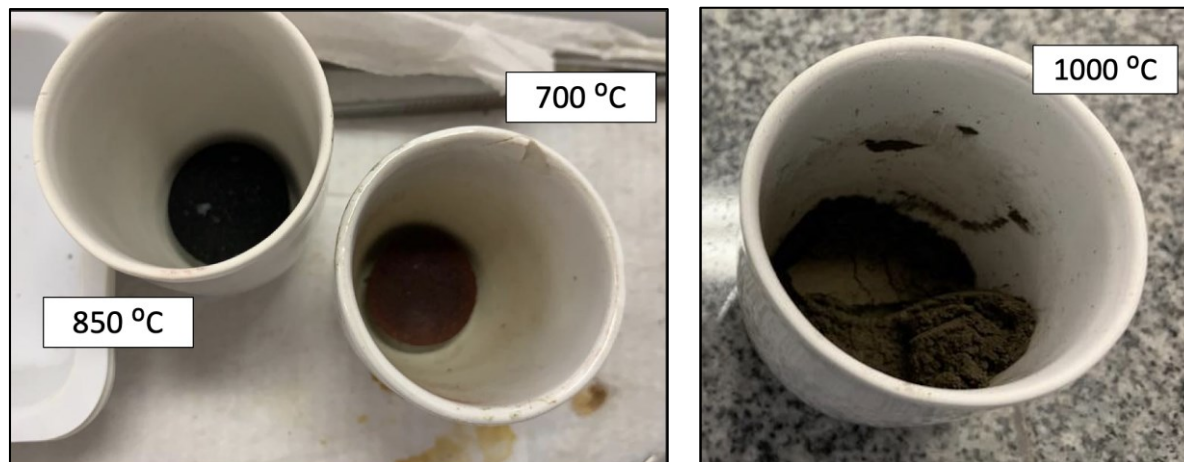
<b>Chemical Name</b>	<b>Formula</b>	<b>Mass (g)</b>	<b>Volume (mL)</b>
Lanthanum Nitrate Hexahydrate	La (NO <sub>3</sub> ) <sub>3</sub> .6H <sub>2</sub> O	4.26	
Nickel Nitrate	Ni (NO <sub>3</sub> ) <sub>2</sub>	1.80	-
Iron Nitrate Nonahydrate	Fe (NO <sub>3</sub> ) <sub>3</sub> .9H <sub>2</sub> O	3.98	
Citric Acid	C <sub>6</sub> H <sub>8</sub> O <sub>7</sub> .H <sub>2</sub> O	11.35	-
EDTA	C <sub>10</sub> H <sub>16</sub> N <sub>2</sub> O <sub>8</sub>	9.54	-
Ammonium Hydroxide 35%	NH <sub>4</sub> OH	-	11.89

Source: Author.

The same ratio of metallic precursors, complexation and chelating agents, and ammonium hydroxide were utilized for the synthesis of LaNiFeO<sub>3</sub> perovskite, which is 1:2:1.1:10. Naturally, however, the increase in the metallic precursors in site A incurred on the increase of the complexing and chelating agents. The resulting mass of the perovskites prepared in these processes was 2.91 g; 2.74 g and 2.55 g, respectively, for the perovskites made in 700 °C, 850 °C and 1000 °C calcination temperatures.

The Figure 10, below, presents a collage of pictures from the three synthesized LNFO catalysts, with the respective calcination temperatures.

Figure 10. Synthesis Steps of  $\text{LaNiFeO}_3$  Perovskites at Different Calcination Temperatures.



Source: prepared by the author.

As shown on the pictures above, greater calcination temperatures seem to induce a darker coloring on the powders obtained after the synthesis. Such characteristic may indicate that a greater metallic content might have been achieved. Additionally, during the final preparation of each perovskite, no significant difference was identified while the powders were being sieved with the 325  $\mu\text{m}$  mesh sieve.

#### 4.3.2 Degradation Kinetics and Catalytic Activity

For the degradation experiments utilizing the synthesized LNFO catalysts from different calcination temperatures, two sets of tests were performed for the evaluation of the degradation capacity of the studied materials.

The first set of experiments involved the application of the LNFO perovskites into a batch reactor with 20 mg/L of phenol, for 180 min, pH 7, and room temperature and atmospheric pressure. This was performed in the same conditions for all perovskites, using 0.3 g of LNFO and a solution of 20 mg/L Phenol and reactor volume of 200 mL.

The second set, however, had the goal to enhance the energy of such system, and provide data on the likely increase of catalytic activity and phenol conversion, with the utilization of a heating platform and temperature of 60  $^{\circ}\text{C}$ . Thus, the utilized LNFO perovskites were tested in the same conditions as the first test, except for the temperature of 60  $^{\circ}\text{C}$ .

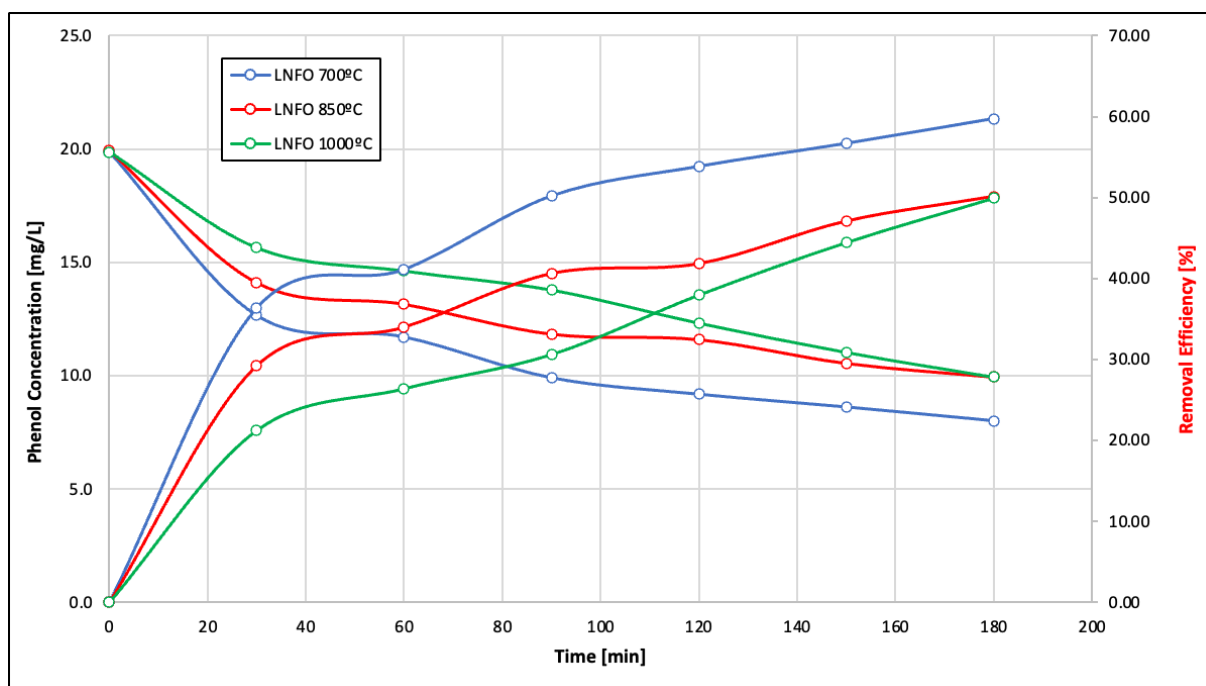
The following section will present and detail the two sets of tests performed with the LNFO perovskites and discuss observed results.

#### 4.3.2.1 Catalytic Performance

After the first set of degradation experiments with the three produced LNFO catalysts, samples of 2 mL were retrieved from the reactor in 0 to 180 min, every 30 min of the entire experiment period, resulting six rounds of samples. Following the sampling, the acquired aliquots were prepared for HPLC analysis, by filtration with 0.22  $\mu\text{m}$  syringe filters, inhibiting any metallic particle to remain in the sample, and then pouring the filtered solution into 20  $\mu\text{L}$  vials, allowing for the analysis of phenol via HPLC.

As such, the Figure 11, presents the responses and results obtained from the HPLC analysis on the synthesized perovskites in its first degradation tests.

Figure 11. First Experiment Results for Phenol Degradation Performance by  $\text{LaNiFeO}_3$  perovskites.



Source: Author.

For the LNFO prepared with the calcination temperature of 700 °C, and based on the response and peak area obtained from the HPLC analysis, as well as its conversion to phenol concentration, it was possible to verify a 59.7% reduction in phenol's initial concentration at 0 min.

As such, it was verified that for the LNFO catalyst calcined at 700 °C, the greatest degradation rate took place on the first 30 minutes of the experiment, with significant decrease in phenol concentration.

The data for the LNFO perovskite calcined at 850 °C has shown a degradation performance of 50.1% in phenol's initial concentration was verified from 0 to 180 min on the experiment.

As seen above, the behavior of LNFO calcined at 850 °C was very similar to the one verified on the first synthesized LNFO, however with a slight decrease in degradation performance.

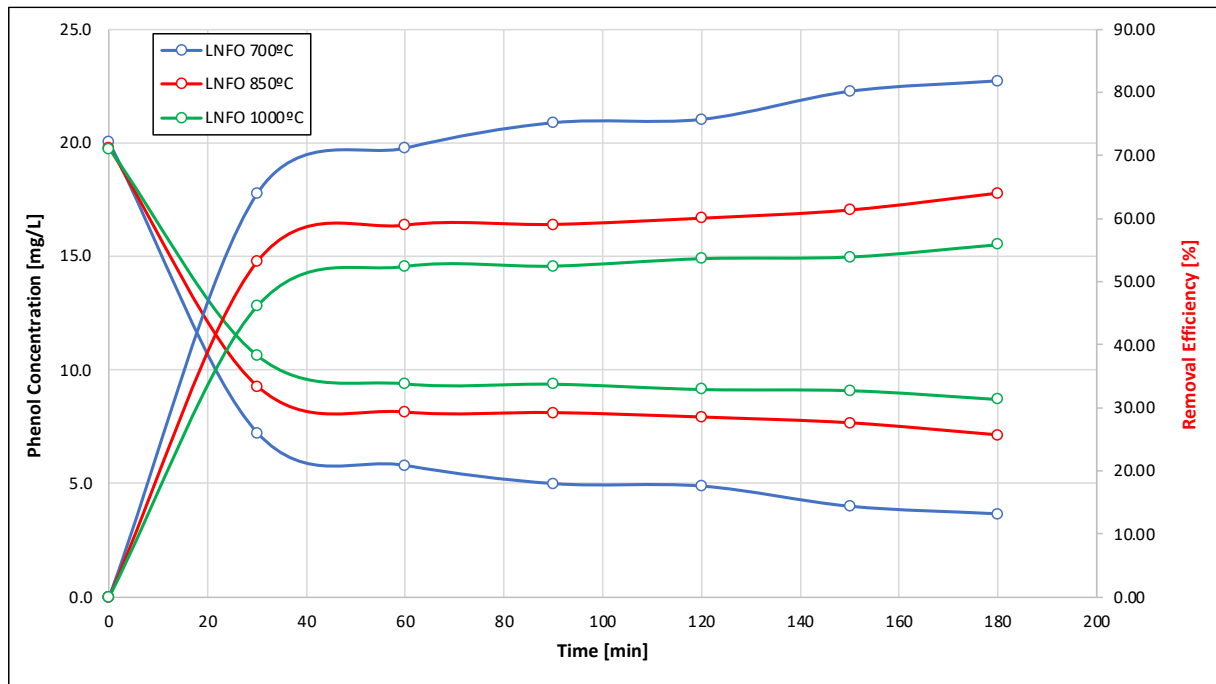
Lastly, for the LNFO prepared at a calcination temperature of 1000 °C, however, similar results were obtained from the HPLC analysis and further conversion, when compared to the LNFO produced at 850 °C, especially, with a degradation performance calculated as 49.9%, from 0 min to 180 min.

By observing the above, when compared to the others LNFO perovskites, it is possible to observe that the degradation rate and trend during the experiment seemed to be less expressive than the ones previously observed for the first 30 min, and subsequently for the entire test until 180 min.

As aforementioned, a second test was performed regarding the synthesized LNFO-perovskites in the different calcination temperatures of 700 °C, 850 °C and 1000 °C. In this second experiment, the same experimental conditions were applied to the studied catalysts, except for the employed temperature, which was of 60 °C. Hence, the experiment had a duration of 180 min, pH 7, absence of any light source and atmospheric pressure, with constant stirring.

The detail the data acquired from the second experiment performed with LNFO perovskites.

Figure 12. Second Experiment Results for Phenol Degradation Performance by  $\text{LaNiFeO}_3$  perovskites.



Source: Author.

Based on the data presented above, a significant degradation performance was observed for LNFO catalyst calcined at 700 °C in relation to Phenol. In this second experiment, the perovskite induced a reduction of 81.8% in the contaminant's initial concentration. This is also approximately 20% higher than the one verified for the first experiment (59.7%). This may be due to the conditions applied in the second experiment, in which a temperature of 60 °C was utilized to heat the batch reactor.

As previously reported by Van-Quoc Truong, 2019, above room temperature systems seem to induce greater ROS formation on the surface of the catalysts, which might result in greater contaminant oxidation. However, data on this matter is yet insufficient.

Conversely, for LNFO perovskite produced at 850 °C, in this test, the LNFO catalyst induced a degradation performance of 64.0% in Phenol's initial concentration of 19.8 mg/L, at 0 min. This represents an increase of approximately 15% in the degradation performance seen for the test in room temperature, which was 50.1%.

The degradation performance observed for the second experiment utilizing LNFO catalyst calcined at 1000 °C showed the lowest increase in degradation performance with the application of heat, and temperature of 60 °C. The reduction observed was of 55.9% in phenol's

initial concentration, representing an increase of only 6% when compared to the first test in room temperature, reported as 49.9%.

It is possible to verify considering the data above that the LNFO catalyst calcined at 700 °C showed significant positive differences from its counterparts for both applied tests. Such scenario is even more evident when analyzing the data for the second experiment, in which a temperature of 60 °C was applied, resulting in the best degradation performance registered in this work. Such findings may indicate also that the use of energy sources not related to light irradiation might increase the formation of ROS in the system and consequently enhance the catalyst's activity.

### **4.3.3 Characterization Techniques**

This section is dedicated to the presentation and discussion of the data acquired from the characterization techniques applied to the  $\text{LaNiFeO}_3$  perovskites synthesized in this study.

Following treatment and assessment of the results obtained from the several degradation experiments performed with all synthesized perovskites (LFO, LTO and LNFO), the group of LNFO catalysts reported the greatest degradation rates and performance.

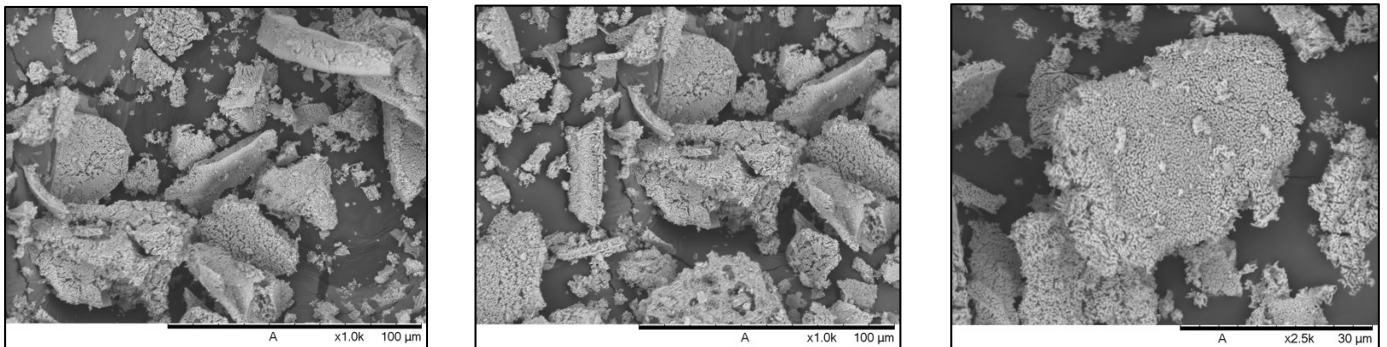
Such findings served as the criteria for the characterization of such catalysts, in order to try to establish correlations between the physical and electrochemical properties of such materials verified by such techniques, and the observed performances.

Thus, the following items will present and discuss the characterization findings in LNFO catalysts analysis.

#### *4.3.3.1 Scanning Electron Microscopy (SEM) and Energy Dispersive X-Ray Spectroscopy (EDS)*

The first characterization technique performed at the synthesized LNFO perovskites were SEM and EDS. The images obtained from SEM analysis are presented below. The images were taken with 1000x and 2500x times zoom.

Figure 13. SEM Pictures obtained at 1000x and 2500x Zoom from  $\text{LaNiFeO}_3$  Perovskite Structure.



Source: Author.

These images are from the LNFO catalyst calcined at  $700\text{ }^{\circ}\text{C}$ , which had the best observed catalytic performance. The images above show the structures formed after the preparation of fresh catalysts. As verified, several major structures are present in the images, as well as smaller portions. These structures have an average size of  $30\text{ to }50\mu\text{m}$ , but also with several other smaller agglomerates, varying in size.

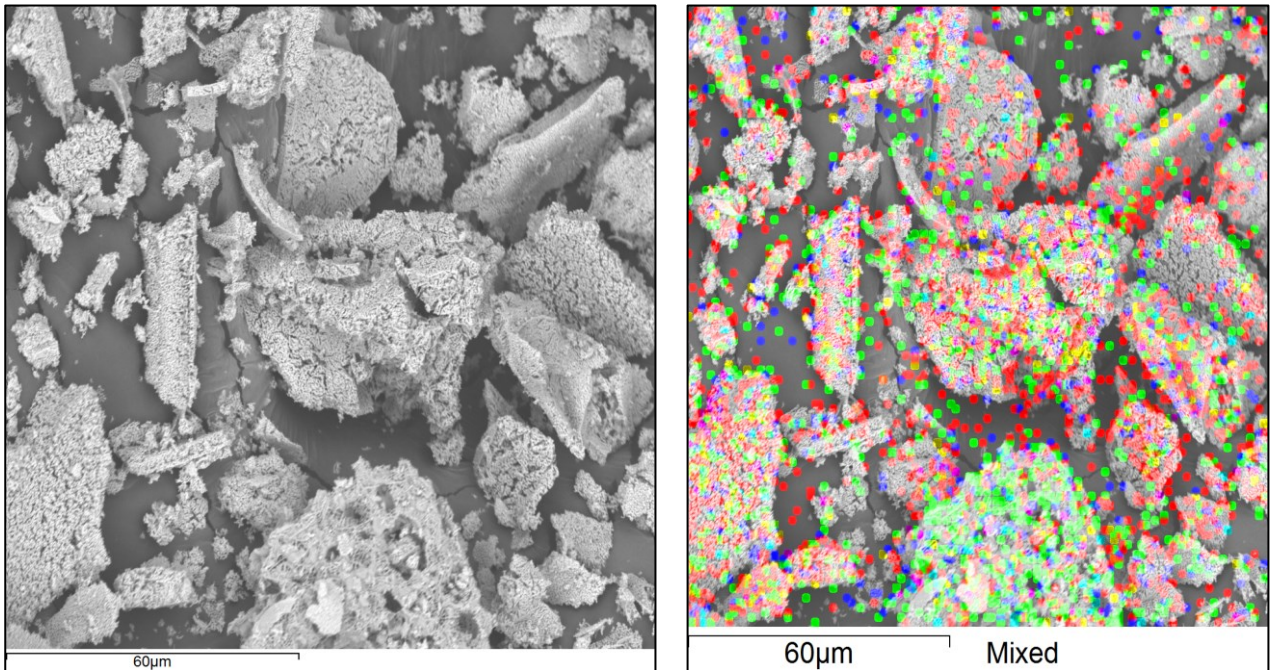
It is also possible to verify, in a qualitative analysis, that the particles focused on the images do have a porous network, what is a positive indicative of likely available sites for the formation of ROS, and the consequent degradation of target contaminants. The third image, zoomed at a rate of 2500x times, particularly focuses on a structure in which it is possible to observe the porous structures in further detail.

As such, the following images also provide further insight on the distribution of the elements present (La, Ni, Fe and O) on each SEM image, through the use of EDS analysis, consisting of a spectroscopy methodology with X-Ray irradiation, in which each unique detected absorbance signature obtained by each present element, results in the identification of such elements. The



Figure 14 shows the distribution of such elements in each obtained image.

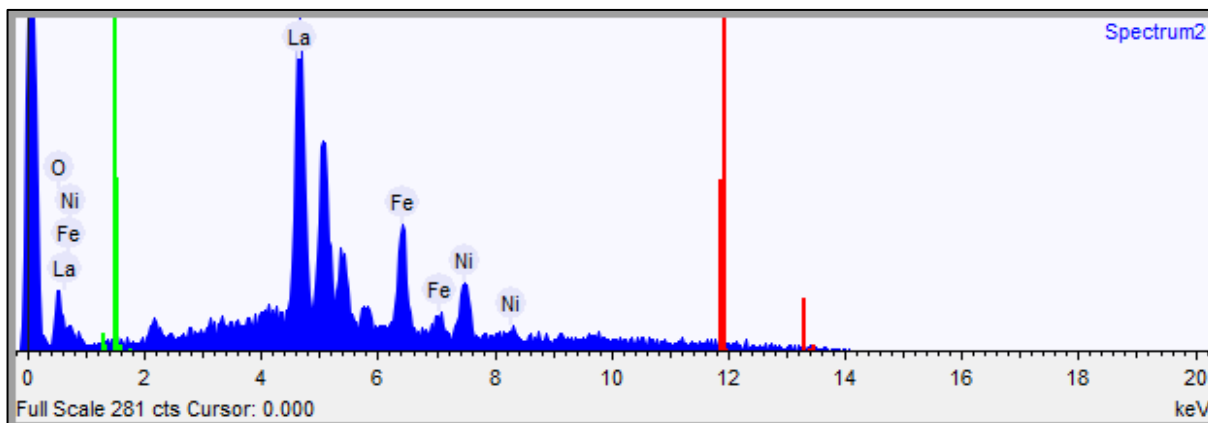
Figure 14. SEM Picture from  $\text{LaNiFeO}_3$  and EDS Analysis.



Source: Author. Note: Lanthanum (Red); Nickel (Blue); Iron (Green).

Based on the images above, it is possible to identify that the elements Lanthanum and Iron represent the majority of elements on the structures observed. This is a positive indicative that the synthesis was successful in its complexation reactions, and that the principal metallic oxides such as Iron and Lanthanum, are abundant within the surface of the catalysts, which may be an important factor of its catalytic performance. Such images were obtained through a voltage of 15 kV, with an image width of 132.6  $\mu\text{m}$ , and resolution of 128x128 pixels.

Thus, the image below also provides quantitative insights of the distribution of the elements discussed, obtained through the spectrum from EDS.

Figure 15. EDS Intensity Spectrum for LaNiFeO<sub>3</sub> perovskite.

Source: LINDEN-UFSC.

As seen in the image above, at 5 keV, a peak is attributed to Lanthanum, what was identified based on its specific absorbance signature. Additionally, the Table 7, below, also computes further data obtained from EDS.

Table 7. EDS Distribution Data for LaNiFeO<sub>3</sub> Perovskite.

Element	Weight %	Atomic %
Lanthanum	64.606	35.915
Oxygen	4.674	22.559
Iron	16.619	22.980
Nickel	14.101	18.546

Source: prepared by the author.

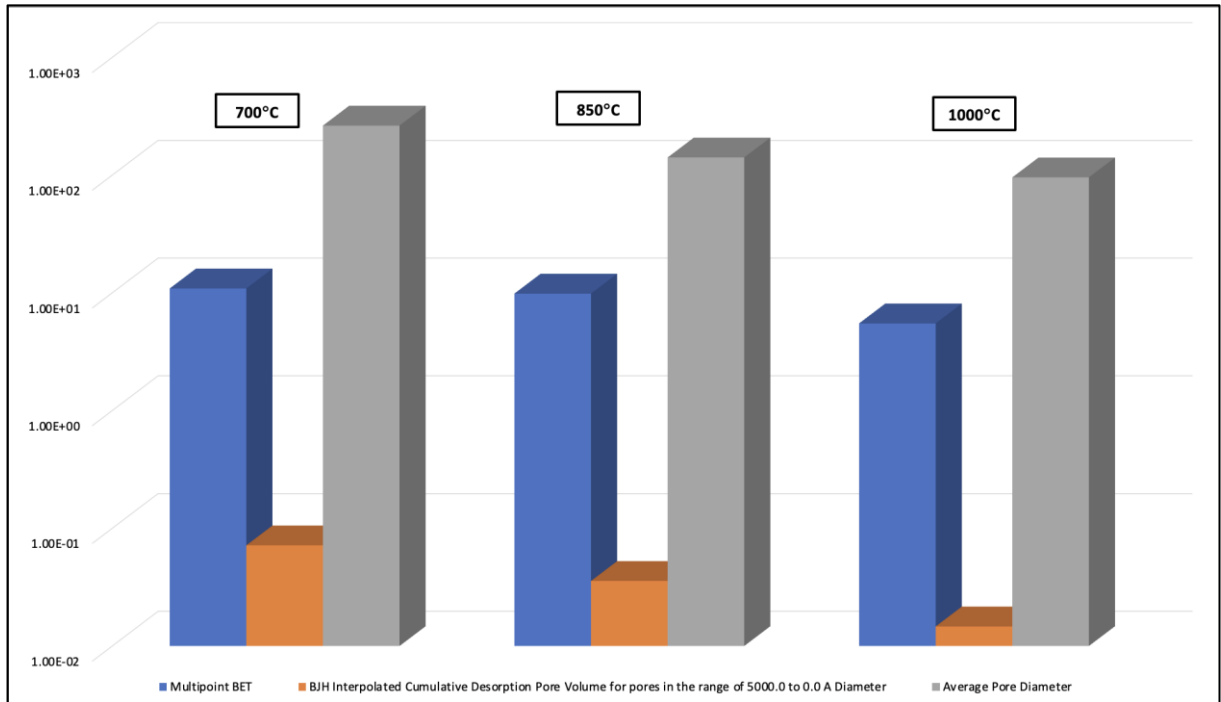
The atomic percentage of Lanthanum in the synthesized catalysts confirms its presence in the structures observed. Hence, its role altogether with Iron atoms facilitate a stable structure, a porous network, and the possibility of ROS formation through the oxidation of the contaminant molecules present.

#### 4.3.3.2 Surface Area (BET)

Brunauer-Emmett-Teller (BET) analysis were performed for the three synthesized LNFO catalysts in order to obtain data on the surface area of the catalysts with best performance. This is made through a multipoint analysis via gas adsorption on the pores of the

structures. The Figure 16, below, shows the results verified for BET analysis for the three LNFO perovskites and its main differences.

Figure 16. BET Results for LaNiFeO<sub>3</sub> Perovskites.



Source: Author.

As seen in the Figure 16, all three parameters evaluated indicated that the perovskite calcined at 700 °C demonstrated higher pore volume, pore size and pore distribution within the structures formed. This might be strong evidence of the behavior of such catalyst, since it also presented the greatest catalytic performance observed in the two experiments carried out in this study, what is likely related to such aspects (LI, et al., 2012).

Moreover, the data observed indicate that surface and pore processes may be stronger while using the 700 °C catalyst, since the target contaminant may more sites to be attached and oxidated through the formation of ROS, as well as its pore sizes, that may store higher masses of the contaminant, also providing more sites and a greater superficial specific area.

#### 4.3.3.3 Zeta Potential (ZP)

Following the data presented and discussed above, Zeta-Potential analysis also provided further insights and evidence on the aspects that differ the catalytic activity of the

synthesized LNFO perovskites. The data is generated based on the measurement of electrostatic repulsion or attraction between particles in a colloidal solution, what indicates the dispersion or stability of suspended materials. Furthermore, Zeta Potential indicates how much of the target contaminant is attached to the surface of the catalyst, or still in suspension, that is, the difference between mobile fluid and fluid that is attached to the catalyst's surface, through potential difference. The Table 8, below, provides data on Zeta Potential parameters obtained for the samples of the catalysts.

Table 8. Zeta Potential Results for LaNiFeO<sub>3</sub> perovskites.

Samples	T	ZP	Mobility	Conductivity	Mean Count Rate
	°C	mV	μmcm/Vs	mS/cm	keps
LaNiFeO <sub>3</sub> (700 °C)	25	-24	-1.883	0.286	50
LaNiFeO <sub>3</sub> (700 °C)	25	-24.4	-1.912	0.289	72
LaNiFeO <sub>3</sub> (700 °C)	25	-25.4	-1.994	0.291	56.7
LaNiFeO <sub>3</sub> (850 °C)	25	20.9	1.64	0.389	36.2
LaNiFeO <sub>3</sub> (850 °C)	25	21.9	1.719	0.372	48.1
LaNiFeO <sub>3</sub> (850 °C)	25	22.3	1.752	0.362	72.3
LaNiFeO <sub>3</sub> (1000 °C)	25	13.6	1.065	0.163	32.7
LaNiFeO <sub>3</sub> (1000 °C)	25	11.9	0.9348	0.154	54.2
LaNiFeO <sub>3</sub> (1000 °C)	25	13.2	1.032	0.151	93.6

Source: Author.

As mentioned above, the ions and its interaction with its mobile phase/fluid, are divided in two parts. The inner region is the ion's surface and highly negatively charged surface, namely the Stern layer, and the outer layer where the attraction is lower, is called the diffuse layer. Such potential between positive and negative particles within these two layers indicate if the suspended materials are in a stable colloidal pattern or if sedimentation processes are occurring (ZHENG, et al., 2019).

As such, the measurement of this potential between layers observed is the Zeta Potential, which indicates the stability of the colloidal solution. The Table 8, above, indicates that all samples not entirely stable colloidal systems, since its Zeta Potential is not either above 30 mV or below -30 mV. However, such measurements are also directly related to the density

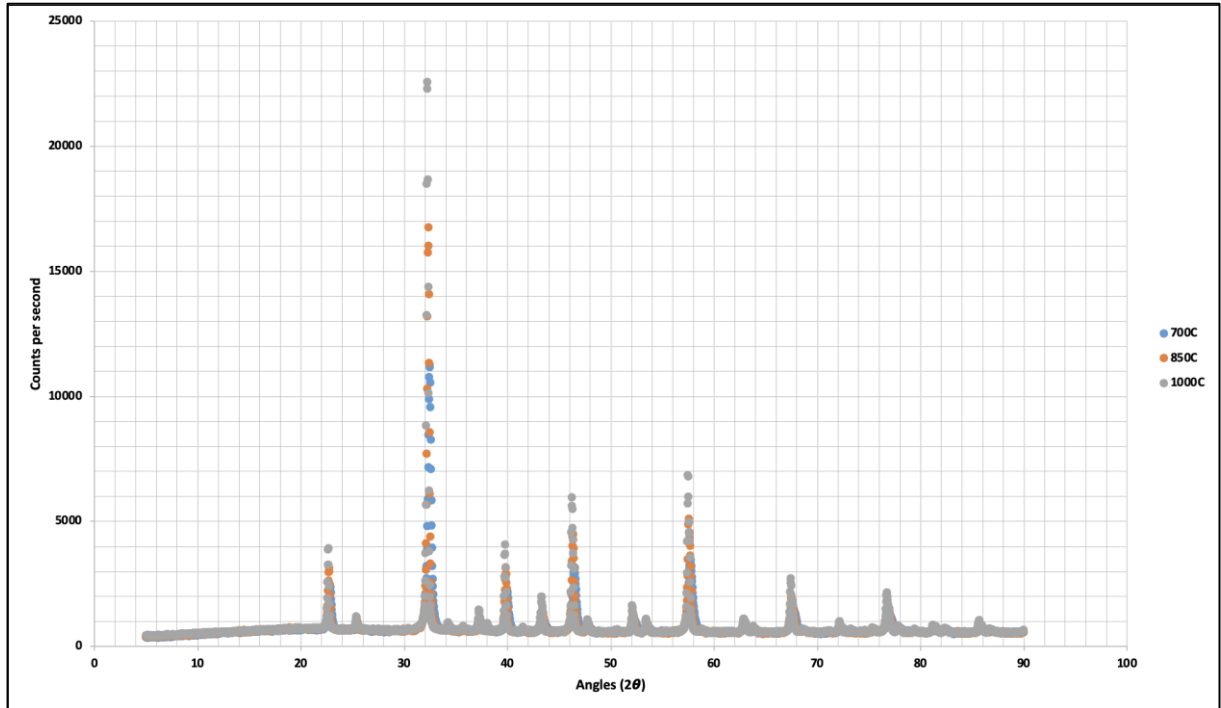
of the mobile fluid, thus, the particles of the studied catalysts might eventually sediment, due to its greater density. Nevertheless, it is likely possible to infer that the samples calcined at 700 °C and 850 °C are more stable than the one calcined at 1000 °C. Moreover, the greater stability of each system indicates that higher repulsive forces are present, when compared to attractive Van der Waals forces, what is ultimately related to the system's resistance to flocculation and further sedimentation as such repulsive forces decrease (YOU, et al., 2019; ZHENG, et al., 2019).

Lastly, the electrical conductivity observed for each sample is related to the thickness ( $k^{-1}$ ) of the double layer of each ion, and its stability. Hence, considering all the discussed data, the sample calcined at 850 °C appears to have the greatest colloidal properties among the other studied catalysts (YOU, et al., 2019; ZHENG, et al., 2019).

#### *4.3.3.4 X-Ray Diffraction (XRD)*

X-Ray Diffraction (XRD) analysis for the three synthesized LNFO catalysts yielded important results on the structure and crystal orientation of studied materials, providing yet further indicatives of the aspects and processes by which each LNFO catalyst employs its catalytic performance. By irradiating X-Ray energy into the studied structures, information is provided through unique absorbance spectrum from each chemical formulation. The

Figure 17. X-Ray Diffraction Data for  $\text{LaNiFeO}_3$  perovskites. , below, showcases the data obtained from XRD.

Figure 17. X-Ray Diffraction Data for LaNiFeO<sub>3</sub> perovskites.

Source: Author.

Based on the data above, it is possible to identify that the LNFO perovskites crystal structure are mainly oriented between 30 and 40° (2θ), as well as the perovskite calcined at 1000 °C showed the greatest reflection of the X-Ray energy inflicted into the structures of the catalysts. This might indicate that less absorbance is related to the number of pores available on each structure, as well as its distribution and size. This is also particularly related to the data observed in EDS, BET and Zeta Potential analyzes, which indicated that the 1000 °C calcined perovskite had less pores (LI, et al., 2012; WU, et al., 2019; HAMMOUDA, et al., 2019).

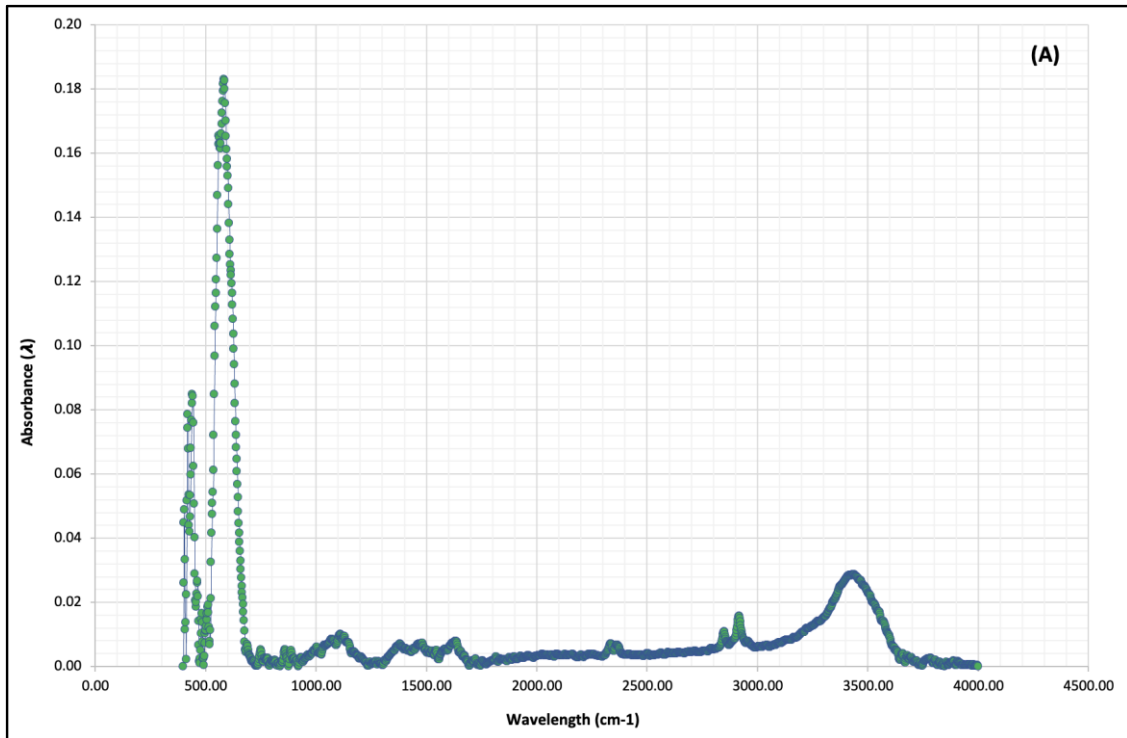
The information acquired from such analyzes are strong drivers for the correlation between the catalytic activity of each perovskite and its physical and electrochemical aspects.

#### 4.3.3.5 Fourier Transform Infrared Spectroscopy (FTIR)

Lastly, the Fourier Transform Infrared Spectroscopy generates data through the unique spectrum formed by the irradiation of Infrared energy into the structures of the catalysts. Such information supports the study of the chemical bonds of the materials tested. The Figures 18 to 20 summarize the patterns observed for the three catalysts.

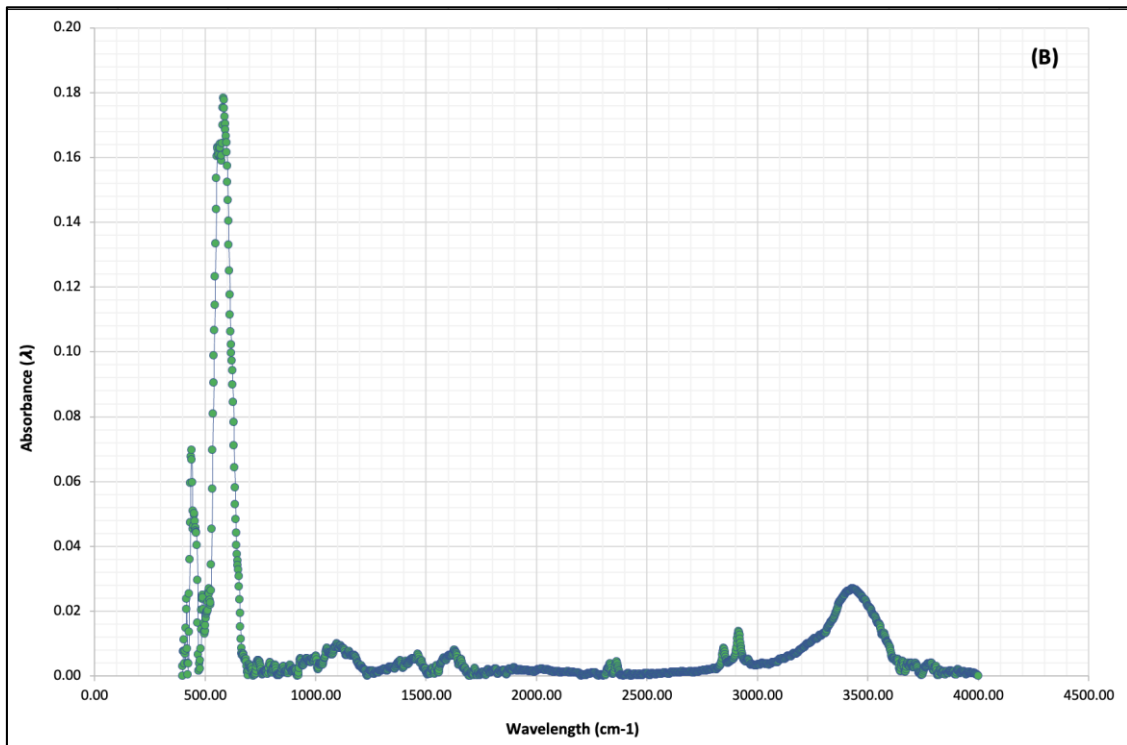


Figure 18. FTIR Results for  $\text{LaNiFeO}_3$  perovskite calcined at  $700^\circ\text{C}$ .



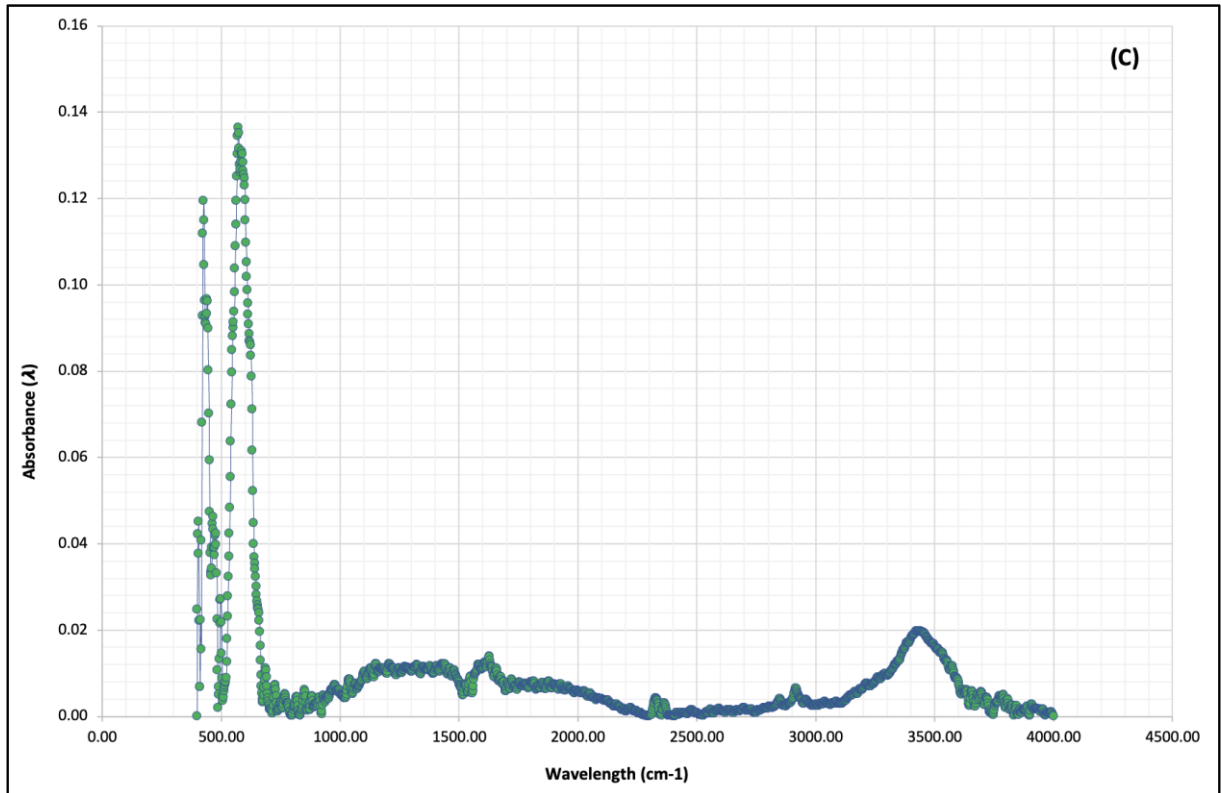
Source: Author.

Figure 19. FTIR Results for  $\text{LaNiFeO}_3$  perovskite calcined at  $850^\circ\text{C}$ .



Source: Author.

Figure 20. FTIR Results for LaNiFeO<sub>3</sub> perovskite calcined at 850 °C.



Source: Author.

As shown on the three displayed graphics, all studied perovskites had its higher peak between 500 and 600  $\text{cm}^{-1}$ , which can be converted to 20,000 nm. However, the highest verified absorbance peak among the studied materials was for the 700 °C calcined catalyst, also with  $\lambda > 0.18$ . This also indicates, altogether with the results observed for all other characterization techniques, that the highest absorbance is related with the number of chemical bonds present in each catalyst. Ultimately, such data is likely related to the quality of the structure in which stable porous aggregates might provide greater catalytic performance.

## 5 CONCLUSIONS AND FINAL CONSIDERATIONS

The main conclusions of this dissertation are:

- The Sol-Gel method paired with the EDTA-Citrate preparation route chosen for the catalyst's preparation was an efficient method for the synthesis of several mixed metallic oxides formulations, in which fine powders were obtained;
- The degradation experiments and its results indicated that dark catalysis might be a cost-effective option for metallic oxides mainly formulated with either Iron or Lanthanum, while Titanium seemed to not provide an acceptable catalytic performance at the conditions tested. Moreover, the use of low heat (60 °C) in the best performing catalysts provided significant results in the degradation of the target contaminants;
- Through the use of SEM and EDS analyzes, it was confirmed that the LNFO catalysts tested had contrasting differences between the calcination temperatures at which they were prepared. However, all catalysts tested had distinct charged surfaces, composed by agglomerates and particles of micrometric size. It also indicated that the studied elements were heterogeneously distributed. BET data further confirms such findings since it was confirmed that the tested catalysts had porous surfaces and networks, with different sizes and distribution. Furthermore, XRD data also shown that that the crystal and mobile phases were successfully identified, whilst FTIR data also indicated differences between the materials tested. Adsorption processes seem to not have a significant role on the degradation mechanism of perovskites;
- The data observed with the best performing catalysts (LNFO) showed that the required aspects for enhanced catalysis processes as well as the formation of ROS, and surface reactions, are mainly present in the studied materials;
- Through the comparison of the data acquired and the data reported in the literature, it is possible to conclude that the synthesized catalysts in this research project are capable of degrading phenolic molecules without the use of light, and at effective degradation rates, in a short period of time and without the use of expensive materials. Additionally, the preparation of the catalysts indicates that the last calcination step at 700 °C might be a better option for the preparation of such catalysts. Finally, this work concludes that the perovskites studied might be relevant materials for the treatment of contaminated waters on the absence of light, and good candidates for next studies at different conditions and organic contaminants.

## **6 SUGGESTIONS FOR FUTURE WORK**

This dissertation provided relevant information on the catalytic performance of heterogeneous mixed metal catalysts (perovskites), which perform in dark conditions. In order to continue to study such materials, the following recommendations are proposed:

- Evaluate the reuse effects in each studied catalyst, and how it's the catalytic performance is affected;
- Identify the oxidative reactive species responsible for the degradation of contaminants, in order to attempt establishing a plausible degradation and reaction pathway on metal oxides;
- Evaluate the remaining toxicity of phenolic solutions after catalytic treatment with all produced catalysts, in comparison to baseline untreated solutions;
- Evaluate the effects of fixed supported beds with different metals in order to enhance catalyst recovery and improve treatment efficacy;
- Further research on the behavior of the catalysts when tested with real contaminated effluents or groundwater; and
- Further research on the mathematical modelling of such catalysts in reactor applications and greener procedures for larger scale production.

## 7 REFERENCES

AIZAT, A., AZIZ, F., MOHD SOKRI, M.N. et al. Photocatalytic degradation of phenol by LaFeO<sub>3</sub> nanocrystalline synthesized by gel combustion method via citric acid route. **SN Appl. Sci.** **1**, 91 (2019). <https://doi.org/10.1007/s42452-018-0104-x>.

ANNAMALAI S, SEPTIAN A, CHOI J, SHIN WS. Remediation of phenol contaminated soil using persulfate activated by ball-milled colloidal activated carbon. **J Environ Manage.** 2022 May 15; 310:114709. doi: 10.1016/j.jenvman.2022.114709.

BESEGATTO, S. V.; CAMPOS, C. E. M.; DA SILVA, A.; GUELLI ULSON DE SOUZA, S. M. A.; ULSON DE SOUZA, A. A.; GÓMEZ, S. Y. Perovskite-based Ca-Ni-Fe oxides for azo pollutants fast abatement through dark catalysis. **Applied Catalysis B: Environmental**, v. 284, n. August 2020, 2021. <https://doi.org/10.1016/j.apcatb.2020.119747>

BIBI, A.; BIBI, S.; ABU-DIEYEH, M.; AL-GHOUTI, M. Towards sustainable physiochemical and biological techniques for the remediation of phenol from wastewater: A review on current applications and removal mechanisms. **Journal of Cleaner Production.** 417. 137810. 10.1016/j.jclepro.2023.137810.

CAI, C.; ZHUOYUE, Z.; LIU, J.; SHAN, N.; ZHANG, H.; DIONYSIOU, D. Visible light-assisted heterogeneous Fenton with ZnFe<sub>2</sub>O<sub>4</sub> for the degradation of Orange II in water. **Applied Catalysis B Environmental.** 2016. 182. 456-468. 10.1016/j.apcatb.2015.09.056.

CANONICA, S.; JANS, U.; STEMMLER, K.; HOIGNE, J. Transformation kinetics of phenols in water: photosensitization by dissolved natural organic material and aromatic ketones. **Environ Sci Technol.** 1995 Jul 1;29(7):1822-31. doi: 10.1021/es00007a020.

COELHO, B. F. E.; NURISSO, F.; BOFFA, V.; MA, X.; RASSE-SURIANI, Fe.; ROSLEV, P.; MAGNACCA, G.; CANDELARIO, V.; DEGANELLO, F.; LA PAROLA, V. A thermocatalytic perovskite-graphene oxide nanofiltration membrane for water depollution. **Journal of Water Process Engineering.** 2022. 49. 102941. 10.1016/j.jwpe.2022.102941.

CHEN, H., MOTUZAS, J., MARTENS, W., Costa, D.C.J. Improved dark ambient degradation of organic pollutants by cerium strontium cobalt perovskite, **Journal of Environmental Sciences**, Volume 90, 2020, Pages 110-118, ISSN 1001-0742. <https://doi.org/10.1016/j.jes.2019.11.013>.

CHEN, D.L., PAN, K.L., CHANG, M.B. Catalytic removal of phenol from gas streams by perovskite-type catalysts, **Journal of Environmental Sciences**, Volume 56, 2017, Pages 131-139, ISSN 1001-0742, <https://doi.org/10.1016/j.jes.2016.04.031>.

DAS, N., KANDIMALLA, S. Application of perovskites towards remediation of environmental pollutants: an overview. **Int. J. Environ. Sci. Technol.** 14, 1559–1572 (2017). <https://doi.org/10.1007/s13762-016-1233-7>

DUTTA, D.; ARYA, S.; KUMAR, S. Industrial wastewater treatment: Current trends, bottlenecks, and best practices. **Chemosphere.** 285. 2021. 131245. [10.1016/j.chemosphere.2021.131245](https://doi.org/10.1016/j.chemosphere.2021.131245).

ESPLUGAS, S.; GIMÉNEZ, J.; CONTRERAS, S.; PASCUAL, E.; RODRÍGUEZ, M. Comparison of different advanced oxidation processes for phenol degradation. **Water Res.** 2002 Feb;36(4):1034-42. doi: 10.1016/s0043-1354(01)00301-3. PMID: 11848342.

GUO, F., Chai, L., ZHANG, S., YU, H., LIU, W., et al. Computational Biotransformation Profile of Emerging Phenolic Pollutants by Cytochromes P450: Phenol-Coupling Mechanism., **Environmental Science & Technology**, 2020 54 (5), 2902-2912. DOI: [10.1021/acs.est.9b06897](https://doi.org/10.1021/acs.est.9b06897)

GARCÍA-MUÑOZ, P., FRESNO, F., LEFEVRE, C., ROBERT, D., KELLER, N. (2020). Synergy Effect Between Photocatalysis and Heterogeneous PhotoFenton Catalysis on Ti-Doped LaFeO<sub>3</sub> Perovskite for High Efficiency Light-Assisted Water Treatment. **Catalysis Science & Technology**. [10.1039/C9CY02269D](https://doi.org/10.1039/C9CY02269D).

HAMMOUDA, S. B.; SALAZAR, C.; ZHAO, F.; LAKSHAMI, D. et al. Efficient heterogeneous electro-Fenton incineration of a contaminant of emergent concern-cotinine- in aqueous medium using the magnetic double perovskite oxide Sr<sub>2</sub>FeCuO<sub>6</sub> as a highly stable catalyst: Degradation kinetics and oxidation products, **Applied Catalysis B: Environmental**, Volume 240, 2019, Pages 201-214, ISSN 0926-3373, <https://doi.org/10.1016/j.apcatb.2018.09.002>.

HEIDINGER, B.; ROYER, S.; ALAMDARI, H.; GIRAUDON, J.-M.; LAMONIER, J.-F. Reactive Grinding Synthesis of LaBO<sub>3</sub>(B: Mn, Fe) Perovskite; Properties for Toluene Total Oxidation. **Catalysts** 2019, 9, 633. <https://doi.org/10.3390/catal9080633>

HUMAYUN, M.; QU, Y.; YAN, R.; ZHIJUN, L.; XULIANG, Z.; JING, L. Exceptional Visible-Light Activities of TiO<sub>2</sub>-Coupled N-Doped Porous Perovskite LaFeO<sub>3</sub> for 2,4-Dichlorophenol Decomposition and CO<sub>2</sub> Conversion. **Environmental Science and Technology**. 2016. 22. 10.1021/acs.est.6b04958.

ISSAKA, E.; NII-OKAI, J.; AMU, D.; YAKUBU, S. et al. Advanced catalytic ozonation for degradation of pharmaceutical pollutants—A review, *Chemosphere*, Volume 289, 2022, 133208, ISSN 0045-6535, <https://doi.org/10.1016/j.chemosphere.2021.133208>.

JAYANTHI, G.; SOWRIRAJAN, S.; KANNAN, K.; GOPAL, A.; MURUGAN, S. A Review on Synthesis, Properties, and Environmental Application of Fe-Based Perovskite. **Advances in Materials Science and Engineering**. 2022. 1-14. 10.1155/2022/6607683.

KIDAK, R.N.; INCE, H. Ultrasonic destruction of phenol and substituted phenols: A review of current research, **Ultrasonics Sonochemistry**, Volume 13, Issue 3, 2006, Pages 195-199, ISSN 1350-4177, <https://doi.org/10.1016/j.ultsonch.2005.11.004>.

KUMAR, A.; KUMAR, S.; BAHUGUNA, A.; KUMAR, A.; SHARMA, V.; KRISHNAN, V. Recyclable, Bifunctional Composites of Perovskite Type N-CaTiO<sub>3</sub> and Reduced Graphene Oxide as an Efficient Adsorptive Photocatalyst for Environmental Remediation. **Mater. Chem. Front.** 10.1039/C7QM00362E.

LI, P.; OUYANG, S.; XI, G.; KAKO, T.; YE, J. The Effects of Crystal Structure and Electronic Structure on Photocatalytic H<sub>2</sub> Evolution and CO<sub>2</sub> Reduction over Two Phases of Perovskite-Structured NaNbO<sub>3</sub>. **The Journal of Physical Chemistry C**. 116. 7621–7628. 10.1021/jp210106b.

LU, X.; QIU, W.; PENG, J.; XU, H.; WANG, D.; CAO, Y.; ZHANG, W.; MA, J. A Review on Additives-assisted Ultrasound for Organic Pollutants Degradation, **Journal of Hazardous Materials**, Volume 403, 2021, 123915, ISSN 0304-3894, <https://doi.org/10.1016/j.jhazmat.2020.123915>.

LUO, X.; SU, C.; CHEN, Z.; XU, H.; L. et al. Mechanochemical synthesis of La-Sr-Co perovskite composites for catalytic degradation of doxycycline in the dark: Role of oxygen vacancies, **Separation and Purification Technology**, Volume 300, 2022, 121891, ISSN 1383-5866, <https://doi.org/10.1016/j.seppur.2022.121891>.

MAINALI, K. Phenolic Compounds Contaminants in Water: A Glance. **Current Trends in Civil & Structural Engineering**. 4. 2020. 10.33552/CTCSE.2020.04.000593.

MAJID, F., RIAZ, S.; NASEEM, S. Microwave-assisted sol-gel synthesis of BiFeO<sub>3</sub> nanoparticles. *J Sol-Gel Sci Technol* 74, 310–319 (2015). <https://doi.org/10.1007/s10971-014-3477-3>.

MIAO, J., SUNARSO, J., SU, C. et al. SrCo<sub>1-x</sub>Ti<sub>x</sub>O<sub>3-δ</sub> perovskites as excellent catalysts for fast degradation of water contaminants in neutral and alkaline solutions. **Sci Rep** 7, 44215 (2017). <https://doi.org/10.1038/srep44215>.

MILL, T.; MABEY, W. **Photochemical transformations**. In: Neely WB, Blau GE, eds. Environmental exposure from chemicals. Vol. 1. Boca Raton, FL: CRC Press, 175-216.



MOHAMMADI, S.; KARGARI, A.; SANAEEPUR, H. et al. Phenol removal from industrial wastewaters: a short review, **Desalination and Water Treatment**, 53:8, 2215-2234, 2014, DOI: [10.1080/19443994.2014.883327](https://doi.org/10.1080/19443994.2014.883327).

NIE Y, ZHANG L, LI YY, HU C. Enhanced Fenton-like degradation of refractory organic compounds by surface complex formation of LaFeO(3) and H(2)O(2). **J Hazard Mater**. 2015 Aug 30; 294:195-200. doi: 10.1016/j.jhazmat.2015.03.065.

NOROUZI, M.; FAZELI, A.; TAVAKOLI, O. Phenol Contaminated Water Treatment by Photocatalytic Degradation on Electrospun Ag/TiO<sub>2</sub> Nanofibers: Optimization by Response Surface Method. **Journal of Water Process Engineering**. 37, 2020, <https://doi.org/10.1016/j.jwpe.2020.101489>.

RAZA, W.; LEE, J.; RAZA, N.; LUO, Y.; KIM, K.H.; YANG, J. Removal of Phenolic Compounds from Industrial Waste Water Based on Membrane-based Technologies. **Journal of Industrial and Engineering Chemistry**. 2019. 71. 1-18. 10.1016/j.jiec.2018.11.024. <https://doi.org/10.1016/j.jiec.2018.11.024>.

ROJAS-CERVANTES, M.L.; CASTILLEJOS, E. Perovskites as Catalysts in Advanced Oxidation Processes for Wastewater Treatment. **Catalysts** 2019, 9, 230. <https://doi.org/10.3390/catal9030230>.

RAYAROTH, M.P.; ARAVIND, U.K.; ARAVINDAKUMAR, C.T. Ultrasound based AOP for emerging pollutants: from degradation to mechanism. **Environ Sci Pollut Res** 24, 6261–6269 (2017). <https://doi.org/10.1007/s11356-016-6606-4>

SINGH, J.; YANG, J.K.; CHANG, Y.Y. Rapid degradation of phenol by ultrasound-dispersed nano-metallic particles (NMPs) in the presence of hydrogen peroxide: A possible mechanism for phenol degradation in water, **Journal of Environmental Management**, Volume 175, 2016, Pages 60-66, ISSN 0301-4797, <https://doi.org/10.1016/j.jenvman.2016.03.025>.

SUN, K. *et al.* Three-dimensional direct lithography of stable perovskite nanocrystals in glass. **Science**. 375,307-310(2022). DOI:[10.1126/science.abj2691](https://doi.org/10.1126/science.abj2691).

TANG, Y., TAO, Y., WANG, Q. *et al.* Mesoporous double-perovskite LaAMnNiO<sub>6</sub> (A = La, Pr, Sm) photothermal synergistic degradation of gaseous toluene. **Journal of Materials Research** **34**, 3439–3449 (2019). <https://doi.org/10.1557/jmr.2019.273>

TARAN, O.; AYUSHEEV, A.; OGORODNIKOVA, O.; PROSVIRIN, I.; ISUPOVA, L.; PARMON, V. Perovskite-like catalysts LaBO<sub>3</sub> (B = Cu, Fe, Mn, Co, Ni) for wet peroxide oxidation of phenol. **Applied Catalysis B: Environmental**. 2015. 180. 10.1016/j.apcatb.2015.05.055. <https://doi.org/10.1016/j.apcatb.2015.05.055>.

VAIANO, V.; MATARANGOLO, M.; MURCIA, J.; ROJAS, H.; NAVIO, J.A.; HIDALGO, M.C. Enhanced photocatalytic removal of phenol from aqueous solutions using ZnO modified with Ag. **Applied Catalysis B: Environmental**. 225. 197-206. 10.1016/j.apcatb.2017.11.075.

WANG, J.; CHEN, H. Catalytic ozonation for water and wastewater treatment: Recent advances and perspective, **Science of The Total Environment**, Volume 704, 2020, 135249, ISSN 0048-9697, <https://doi.org/10.1016/j.scitotenv.2019.135249>.

WANG, K., HAN, C., SHAO, Z. P., QIU, J. S., WANG, S. B., LIU, S. M. Perovskite Oxide Catalysts for Advanced Oxidation Reactions. **Adv. Funct. Mater.** 2021, 31, 2102089. <https://doi.org/10.1002/adfm.202102089>.

WANG, H.; ZHANG, L.; HU, C.; WANG, X.; LYU, L.; SHENG, G. Enhanced degradation of organic pollutants over Cu-doped LaAlO<sub>3</sub> perovskite through heterogeneous Fenton-like reactions, **Chemical Engineering Journal**, Volume 332, 2018, Pages 572-581, ISSN 1385-8947, <https://doi.org/10.1016/j.cej.2017.09.058>.

WEI, K.; FARAJ, Y.; YAO, G.; XIE, R.; LAI, B. Strategies for improving perovskite photocatalysts reactivity for organic pollutants degradation: A review on recent progress,

**Chemical Engineering Journal**, Volume 414, 2021, 128783, ISSN 1385-8947, <https://doi.org/10.1016/j.cej.2021.128783>.

WETCHAKUN, K.; WETCHAKUN, N.; SAKULSERMSUK, S. An overview of solar/visible light-driven heterogeneous photocatalysis for water purification: TiO<sub>2</sub>- and ZnO-based photocatalysts used in suspension photoreactors. **Journal of Industrial and Engineering Chemistry**. 2018. 71. 10.1016/j.jiec.2018.11.025.

WU, S.; LIN, Y.; YANG, C.; DU, C.; TENG, Q.; MA, Y.; ZHANG, D.; NIE, L.; ZHONG, Y. Enhanced activation of peroxymonosulfate by LaFeO<sub>3</sub> perovskite supported on Al<sub>2</sub>O<sub>3</sub> for degradation of organic pollutants, **Chemosphere**, Volume 237, 2019, 124478, ISSN 0045-6535, <https://doi.org/10.1016/j.chemosphere.2019.124478>.

YOU, M.S.; HEO, J.H.; PARK, J.K.; MOON, S.H.; PARK, B.J.; IM, S.H. Low temperature solution processable TiO<sub>2</sub> nano-sol for electron transporting layer of flexible perovskite solar cells, **Solar Energy Materials and Solar Cells**, Volume 194, 2019, Pages 1-6, ISSN 0927-0248, <https://doi.org/10.1016/j.solmat.2019.02.003>.

ZHU, H.; ZHANG, P.; DAI, S. Recent Advances of Lanthanum-Based Perovskite Oxides for Catalysis. **ACS Catalysis**. 5. 150921141639007. 10.1021/acscatal.5b01667.